Chapter 7
Evaluating Discharge Regimes of Karst Aquifer

Peter Malík

Karst springs are typical for abrupt changes of discharge immediately following recharge events. Monitored discharges of springs are used to determine quantitative variability over the period of time, showing their reliability as dependable water sources.

Karst aquifers also exhibit (at least) dual groundwater flow regimes, that is, fast (conduit-dominated) flow and slow (diffuse) flow. This is something that can be observed in nature as the fast change of water amount outflowing from the groundwater source, or described by rapidly responding hydrographs, recording water levels or discharges. Selection of proper investigative techniques characterising discharge regime properties of a karst aquifer is therefore important in order to identify possible theoretical background models describing this behaviour. On this basis, we can also find a particular method of hydrograph separation into flow components linked to the fast-flow regime, slow-flow regime or intermediate regimes as well. With this point in mind, several quantitative methods that might be particularly useful in hydrograph analysis of water outlets from the karst aquifer system are briefly discussed here.

7.1 Discharge Regime: Definition, Typical Karstic Manifestations

In hydrogeology and hydrology, a term "regime" refers to the changing conditions of (ground) water phenomenon, its characteristic behaviour or prevailing system of natural processes which are usually observed in regular pattern of occurrence.

P. Malík (✉)
Geological Survey of Slovak Republic, Mlynská dolina 1, 817 04, Bratislava, Slovakia
e-mail: peter.malik@geology.sk

Z. Stevanović (ed.), *Karst Aquifers – Characterization and Engineering*,
Professional Practice in Earth Sciences, DOI 10.1007/978-3-319-12850-4_7

Nature of temporal changes during time-varying aquifer characteristics, in particular groundwater level, but also physical and chemical properties of groundwater, studied in relation to the factors that affect and determine it is a frequent subject of hydrogeological studies. Regular pattern of discharge changes, a discharge regime, typical for individual springs or river basins, is used for their characterisation and distinction. The term "discharge regime" means the regular, expected discharge of flowing water within a year. For example, watersheds in alpine regions may have snowmelt-dominated or glacier-dominated discharge regime, while in great lowland basins the discharge regime can be described as rain or monsoon dominated. Karst aquifers, due to their ability of groundwater flow concentration, are clearly recognisable in their discharge regime characteristics.

Immediate and ultra-intensive discharge response to recharge impulses manifested in hydrographs as steep peaks with enormous amplitudes is typical for wide range of karstic springs (Fig. 7.1). This feature is caused by a significant shift of transmissivity values of karstic rocks towards high levels contrary to other aquifer types (intergranular or fissure permeability). On the other hand, specific yield (storativity) values of rock types prone to karstification are not different, or are even lower than in other aquifers.

High values of hydraulic diffusivity parameter (ratio of transmissivity and specific yield) are then reflected in typical spiky shape of karst hydrographs. Even spring situated in granites and its debris, with apparently shallow groundwater circulation, can better absorb and buffer occasional recharge inputs due to relatively higher storage capacity and relatively lower hydraulic conductivity (Fig. 7.2). We should note that the two springs for which hydrographs were depicted in Figs. 7.1 and 7.2 are approximately 15 km away from each other, and hydrographs show

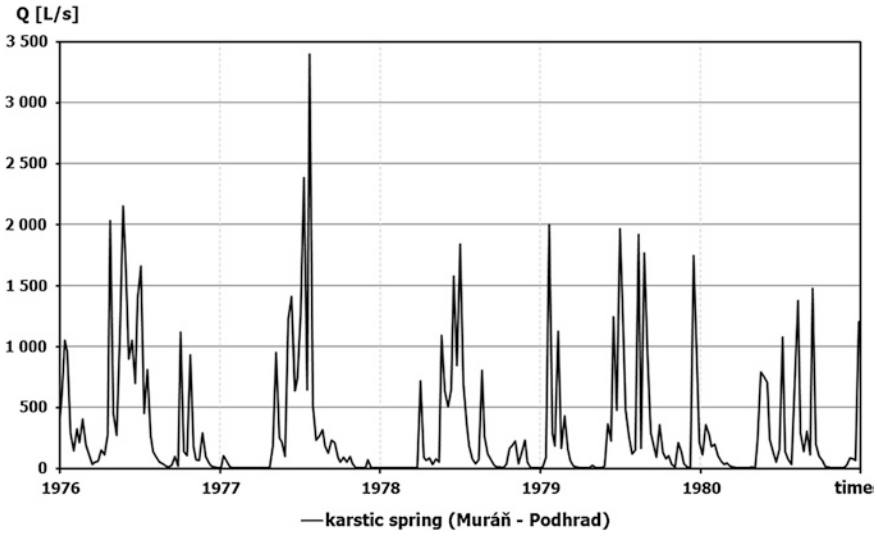

Fig. 7.1 Typical quantitative behaviour of a karstic spring (Podhrad spring in Muráň municipality, Central Slovakia)

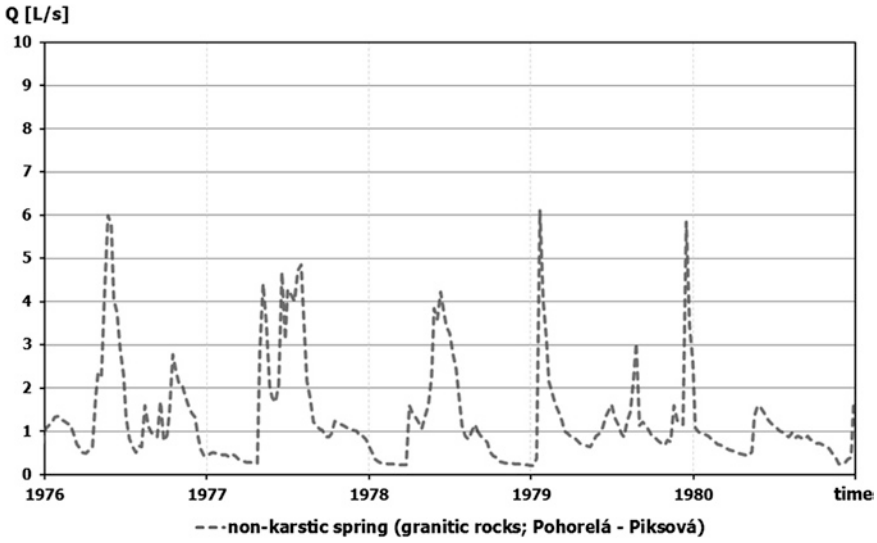

Fig. 7.2 Typical quantitative behaviour of a non-karstic spring (Piksová spring in Pohorelá municipality, Central Slovakia)

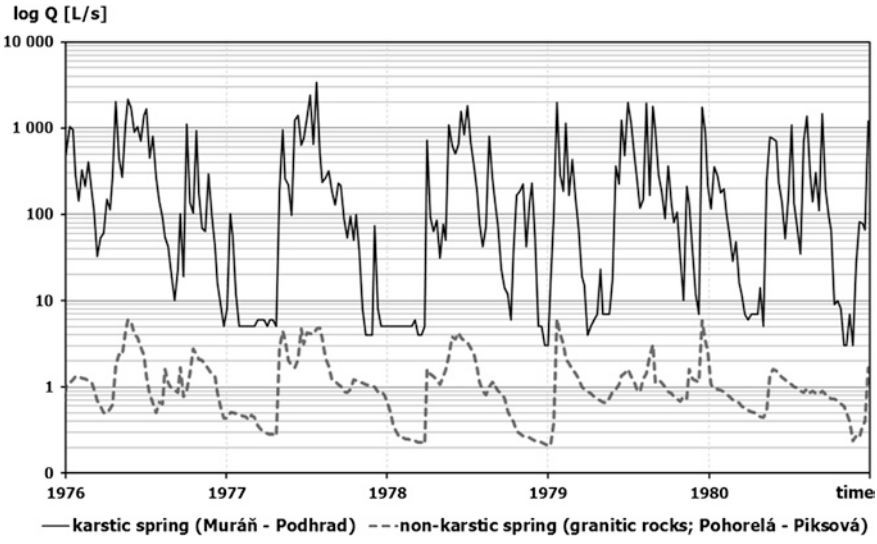

Fig. 7.3 Comparison of discharge regime patterns of a karstic (Fig. 7.1) and non-karstic (Fig. 7.2) spring on a semilogarithmic plot

response to nearly the same course of precipitation episodes. The karstic spring (Fig. 7.1) is the Podhrad spring in Muráň municipality (Central Slovakia), and the one with groundwater circulation in crystalline rocks is named Piksová near the village of Pohorelá, both with weekly measured data in the period of 1976–1981 period. To compare the responses of springs with different regimes, sometimes,

it is better to use a logarithmical plot of discharge versus time as in the case of Fig. 7.3, so in one view, you can see the comparison of the two values without having to adjust the scale on the *y* axis. The usefulness of logarithmical plots of discharge (Q) values will be presented also later, but here in Fig. 7.3 one can see an unstable behaviour of karstic spring with strong reaction to every precipitation impulse, while weathered crystalline aquifer response only to major recharge events.

7.2 Spring Discharge Variability

Discharge of spring changes in time, due to the recharge and emptying of its natural reservoir. The amplitude and frequency of discharge changes are also dependent on aquifer geometry and physical properties, and karstic springs are typical for abrupt and significant changes of discharge. However, from the water management point of view, such instability is less welcome and temporal changes of spring's discharge should be classified before undertaking a serious water management investment. One should keep in mind that proper quantitative description of spring cannot be based on a single measurement of discharge or several sporadic data from different periods. Estimation of discharge variability parameter requires multiple measurements. Systematic measurements of discharge should be performed at least for one complete hydrological cycle where both regular major recharge events and recession are observed. Gauging frequency of groundwater sources was recommended to be at least once a week, but only daily measurements are capable of recording rapid changes of discharge in the case of karstic springs. Having a possibility of automatic electronic discharge recording nowadays, the problem of gaps in discharge time series is less actual than before. More pronounced problem today is the resolution of measurement. The shape of gauging weirs of karstic springs should enable precise reading in both low-water stages, when the discharge falls to several litres per second, and the high-water stages when several cubic metres per second flow through the same gauging object. The V-notch weirs (Thomson weir is a V-notch weir of 90° angle) are better in low-water stages, but these are not able to cope with high flow rates. For high-water stages, rectangular shapes of weirs (Poncelet weirs) of sufficient width can be used, and sometimes, the combination of both V-notch and rectangular shapes is used (Fig. 7.4a, b) for enhancing the capability of both extreme readings. As a better option, combination of several (two or three) V-notch weirs with gradually more opened angle towards outer edges (Fig. 7.4d) can be used. Hydraulic behaviour of this type of weir is said to be better theoretically described than that in Fig. 7.4a, b. Parshall flume (Fig. 7.4c) can be used if there is limited vertical space for achieving downflow gradient, but its accuracy is lower than that of previously mentioned sharp-crested weir allowing water to fall cleanly down from the weir.

According to their changes of discharge, we can distinguish perennial springs that will never get dry (where their discharges are always higher than zero) and

Fig. 7.4 Various types of weirs used for discharge gauging of karstic springs **a** combined Thomson (*V-notch*) and Poncelet (*rectangular*) weir—dry period; **b** combined Thomson (*V-notch*) and Poncelet (*rectangular*) weir—wet period; **c** Parshall flume; and **d** combined V-notch weir

ephemeral (intermittent) springs that discharge groundwater in irregular time intervals. Intermittent springs discharge only for a period of time reflecting the aquifer recharge pattern, while at other times they stay dry. An interesting case is the phenomenon of periodic springs (ebb-and-flow springs; "rhythmic" springs). These springs are regularly discharging approximately the same amount of water in short time intervals; their discharge time series are oscillating for at least a certain period of time. In the past, these were connected to existence of a siphon that fills up and empties out with certain regularity, irrespective of the recharge pattern (Kresic 2007). Mangin (1969) explained this phenomenon as a result of emptying a water reservoir through two differently situated pipes, which fits also to the model proposed by Oraseanu and Iurkiewicz (2010), and Bonacci and Bojanic (1991) had suggested a mathematical working model of such a spring function consisting of two reservoirs joined by a siphon. We can classify the spring as being periodic if its discrete emptying mechanism is working at least in some specific hydrological stages. Appearance of periodic springs is typical especially for karstic regions elsewhere in the world.

Classification of springs based on average discharge rate can be geographically dependent as springs—natural groundwater sources—are differently perceived and understood according to water scarcity or profusion in different parts of the world. Meinzer's classification (1923b) shown in Table 7.1, however, can serve as the first reference point.

Table 7.1 Classification of spring's magnitude according to average annual discharge after Meinzer (1923b)

Magnitude of spring's discharge	Average annual discharge (Q) in [L/s]
1st—first	>10,000
2nd—second	1,000–10,000
3rd—third	100–1,000
4th—fourth	10–100
5th—fifth	1–10
6th—sixth	0.1–1
7th—seventh	0.01–0.1
8th—eighth	<0.01

Without specifying other discharge parameters, classification based on average discharge is not very useful as the statistical distribution of discharge values (especially in karst) is often lognormal. The overall discharge average value may be influenced by several massive flood events, while for the rest of the period, the spring discharges only small amounts of water or may dry out. In many countries, spring classification is based on minimal discharge data (Kresic 2007), but sometimes maximum discharges are useful for karst hydrological modelling (Bonacci 2001). However, when evaluating availability of water for potential spring utilisation, it is important to estimate a measure of spring's discharge variability. Spring discharge monitoring data should be used to determine spring discharge variability over the period of study for individual spring. Classification of spring's discharge variability is used to characterise trends in low-flow periods and in combination with mean annual discharge to estimate the category of total annual discharge. Discharge variability can be also used to estimate regional hydrogeological processes and hydraulic properties of aquifers. Springs with high discharge variability can indicate high degree of transport properties of the aquifer and quick response of the system to recharge.

Presented methods of classification of spring's discharge variability are based on statistical parameters of regularly measured discharges. The simplest measure of spring's discharge variability is the ratio of maximal and minimal recorded discharge (Q_{max}/Q_{min}), what may be defined as index of variability I_v (Eq. 7.1)

$$I_v = \frac{Q\text{max}}{Q\text{min}} \tag{7.1}$$

Springs with the I_v values greater than 10 are considered highly variable, and those where index of variability is less than 2 are sometimes called constant or steady springs (Kresic 2007). Based on comparison of maximal and minimal recorded discharge, some other (classical) classifications of springs by discharge variability (Dub and Němec 1969; Netopil 1971) may be as follows. Index of variability here can be classified into several degrees of spring's reliability (Table 7.2).

Slovak Hydrometeorological Institute, responsible for observations of more than 1,300 springs since 1960s, uses the same index of variability I_v (Eq. 7.1) for characterisation of spring's discharge stability as shown in Table 7.3.

Table 7.2 Degrees of spring's discharge reliability based on index of variability I_v value (Dub and Němec 1969; Netopil 1971)

Degree of spring's reliability	I_v (Q_{max}/Q_{min})
Excellent	1.0–3.0
Very good	3.1–5.0
Good	5.1–10.0
Modest	10.1–20.0
Bad	20.1–100.0
Very bad	>100.0
Ephemeral spring	∞

Table 7.3 Degrees of spring's discharge reliability based on I_v (index of variability) value as applied in the Slovak Hydrometeorolgical Institute

Degree of spring's discharge stability	I_v (Q_{max}/Q_{min})
Stable	1.0–2.0
Unstable	2.1–10.0
Very unstable	10.1–30.0
Totally unstable	>30.0

It is clear that with longer observation period, the more extreme hydrologic phenomena can be recorded (higher floods, longer droughts) and accordingly, spring's reclassification can lead only to "less reliable" degrees.

To reduce the influence of extreme outliers on spring's classification, other statistical parameters of discharge time series can be employed. We should always keep in mind that a simple arithmetical mean (average) is the "worst characterization parameter" as in the case of high discharge amplitude, typical for karstic springs, it emphasizes the large discharges that occur only several times a year. Instead of using arithmetical mean, the use of median value is more recommended in the case of karstic springs, together with other parameters characterizing the variability of discharge changes.

Meinzer (1923b) proposed a measure of spring variability V expressed in percentage (Eq. 7.2):

$$V = \frac{Q_{max} - Q_{min}}{\emptyset} \times 100\,(\%) \tag{7.2}$$

where

V is the spring variability index expressed in %,
Q_{max} and Q_{min} are maximal and minimal recorded discharge and
Φ is the arithmetical mean of spring discharge values.

If $V < 25$ %, we can speak about *constant* spring discharge, for *variable* spring the $V > 100$ %.

The spring variability coefficient (SVC; Eq. 7.3) is based on comparison of the discharges with 10 and 90 % exceedence; spring coefficient of variation parameter (SCVP; Eq. 7.4) is based on standard deviation and arithmetical mean of spring discharge values.

$$\mathrm{SVC} = \frac{Q_{10}}{Q_{90}} \tag{7.3}$$

where SVC is spring variability coefficient, Q_{10} is a discharge value which is exceeded in 10 % of the time and Q_{90} is discharge which is exceeded in 90 % of the time (see part on flow duration curves (FDCs) for definition of exceedence). Spring's classification according to SVC (Flora 2004; Springer et al. 2004) shown in Table 7.4 is based on works by Meinzer (1923a), Netopil (1971) and Alvaro and Wallace (1994).

Also Slovak technical standard STN 751520 (SÚTN 2009; Table 7.5) quantifies "spring's discharge stability" according both to Q_{max}/Q_{min} ratio (index of variability I_v) and to the *SVC* (Q_{10}/Q_{90}).

Flora (2004) and Springer et al. (2004) proposed also SCVP, calculated according to Eq. 7.4.

$$\text{SCVP} = \frac{\sigma}{\emptyset} \tag{7.4}$$

where SCVP is spring coefficient of variation parameter, σ is standard deviation of spring discharge values and Φ is the arithmetical mean of spring discharge values. Variability classes according to SCVP are then classified as shown in Table 7.6.

Table 7.4 Classification of springs by discharge using *SVC* (Flora 2004; Springer et al. 2004)

Spring's classification	Spring variability coefficient (SVC)
Steady	1.0–2.5
Well balanced	2.6–5.0
Balanced	5.1–7.5
Unbalanced	7.6–10.0
Highly unsteady	>10.0
Ephemeral	∞

Table 7.5 Degrees of spring's discharge stability based on index of variability (I_v) or spring variability coefficient (*SVC*) (SÚTN 2009)

Degree of spring's discharge stability	Value of SVC or I_v
Very stable	1.0–3.0
Stable	3.1–10.0
Unstable	10.1–20.0
Very unstable	20.1–100.0
Extremely unstable	>100.0

Table 7.6 Classification of springs by discharge using spring coefficient of variation parameter (SCVP) (Flora 2004; Springer et al. 2004)

Spring's classification	Spring coefficient of variation parameter (SCVP)
Low	0–49
Moderate	50–99
High	100–199
Very high	>200

7.3 Flow Duration Curve

The FDC is a measure of the range and variability of a stream's flow or spring's discharge. The FDC represents the percentage of time during which specified flow rates/discharges are exceeded at a given location (Foster 1924, 1934; Searcy 1959). This is usually presented as a graph of flow rate (discharge) versus percentage of time at which flows are greater than, or equal to, that flow. Although the FDC does not show the chronological sequence of flows, it is useful for many studies. The FDC submits one of the most fundamental pieces of information about the discharge regime of karstic springs. While many past discharge regime classifications were using only comparison discharge minima and maxima to estimate the "stability of discharge", the FDC enables more detailed insight into the mode of spring's quantitative behaviour. To construct a reliable FDC, one needs sufficiently long set of regular observations, at least to cover the whole annual hydrological cycle (both recharge period and period of recession). The data in the discharge time series should be then simply ordered according to the size, from highest to lowest. The data are then plotted against a "percentage exceedence" scale. Each percentage exceedence increment is 100 % divided by the number of data points (dataset population, or number of measurements). If there are 365 discharge measurements, each regularly taken every day within 1 year, and if the discharge data are organised from highest to lowest, the percentage exceedence of the first datum (maximum) will be 1/365 = 0.27 %. The twelfth highest discharge from the dataset would have percentage exceedence of 12/365 = 3.29 %, while for the 279th discharge from the maximum it is 279/365 = 76.44 %. Percentage exceedence can be added as a new data column to show at what percentage exceedence each discharge occurred.

After the FDC was constructed, it can serve as a reference object for the spring discharge. If we look at the discharge value at "50 % exceedence", we will see the value that corresponds to the median value of discharge. If the value of "70 % exceedence" is perhaps 147 L/s, this does not mean that the discharge is 147 L/s for 70 % of the time, but that the discharge is equalled or exceeded for 70 % of the time. In other words, the discharge is at this value or at a higher value for 70 % of the time. If we look at the discharge at 20 % exceedence and it is 700 L/s, this is a higher flow rate, so the discharge is only at or greater than this value for a smaller proportion of the year. If we look at 100 % exceedence and it is perhaps 25 L/s which is the lowest discharge recorded, so by definition, the discharge of the spring is at this value or more for 100 % of the time.

Discharge (flow rate) is often referred to as Q, and the exceedence value as a subscript number, so Q_{95} means the discharge equalled or exceeded for 95 % of the time. Q_{50} is then equal to median value of discharge, but the average or mean flow rate Q_{mean}, and the arithmetic mean of all of the discharges in the dataset usually occurs between Q_{20} and Q_{40}, depending on how "flashy" or "steady" the spring being analysed is. Flow rates between Q_0 and Q_{10} are considered high flow rates, and Q_0 to Q_1 would be extreme flood events. Discharges from Q_{10} to Q_{70} would be of the medium range, while discharges from Q_{70} to Q_{100} are the "low flows" when

Table 7.7 Example of the discharge exceedence table for two karstic springs

Spring	Q_1	Q_5	Q_{10}	Q_{20}	Q_{30}	Q_{40}	Q_{50}	Q_{60}	Q_{70}	Q_{80}	Q_{90}	Q_{95}	Q_{99}
Brúsik	70.0	29.0	20.0	14.4	10.8	8.4	7.1	6.1	4.6	3.8	2.9	2.0	0.9
Vlčie bralo	29.1	26.2	24.0	21.6	19.7	15.6	15.2	14.7	14.7	13.7	10.6	9.7	9.3

Brúsik with pure limestones in its recharge area, Vlčie bralo dewaters dolomitic limestones. Discharge data are in L/s

waterworks will be in a need of water, and should take into account these values for securing available groundwater amounts. As we move further to the right on the FDC, water supply systems will begin to shut down due to low flow. As discharges move from Q_{95} towards Q_{100}, we would be facing the low-flow droughts. It is usual to present the discharge exceedence values in the tables where the most interesting reference points are more densely scaled at both the sides of the exceedence percentages (Q_1; Q_5; Q_{10} … Q_{90}; Q_{95}; Q_{99}), while the bulk is shown with the 10 % step. An example of the discharge exceedence table for the two karstic springs with similar values of the mean discharge is shown in Table 7.7. Available (exploitable) discharge amounts are then related—based on legislation or regional experience—as discharges with 70–90 % exceedence, i.e. Q_{70} or Q_{90}, usually Q_{80}, for securing water availability in the respective period of the year.

Another form of showing the discharge exceedence value is the so-called M-day discharge or M-day continuous discharge during low-water period where the exceedence value is given in the number of days throughout the year: 300-day exceedence then corresponds to 82.19 % exceedence (as is equal to 300/365) or 355-day exceedence corresponds to 97.26 % (=355/365). This means that 330-day discharge is statistically secured for 330 days annually—in other words that during 330 days within a year, the discharge of the spring is higher or at least equal to this value. We should bear in mind that many authors use the same way of showing the exceedence values as they were shown in percentages (e.g. Q_{90} for 90-day exceedence), and we should carefully check the author's attitude to distinguish the meaning of the values. Usually, the description of discharge exceedence exceeding the value of 100, such as Q_{300}, reveals that the "M-day discharge" format was applied.

The shape of the FDC is determined by hydraulic characteristics and geometrical shape of the aquifer and the recharge area, and the curve may be used to study these characteristics or to compare the characteristics of spring with those of another. A curve with a steep slope throughout denotes a highly variable spring whose discharge is largely from karstic conduits, whereas a curve with a flat slope reveals the presence of better groundwater storage capacity, which tends to equalise the flow. The slope of the lower end of the FDC shows the characteristics of the perennial storage in the recharge area; a flat slope at the lower end indicates a large amount of storage, and a steep slope indicates a negligible amount. Springs whose high discharges come mainly from snowmelt tend to have a flat slope at the upper end. The same is true for springs with large epikarst storage or those that are connected to surface water inputs draining swamp areas. An example of the FDC for the two karstic springs shown in Table 7.7 is shown in Fig. 7.5.

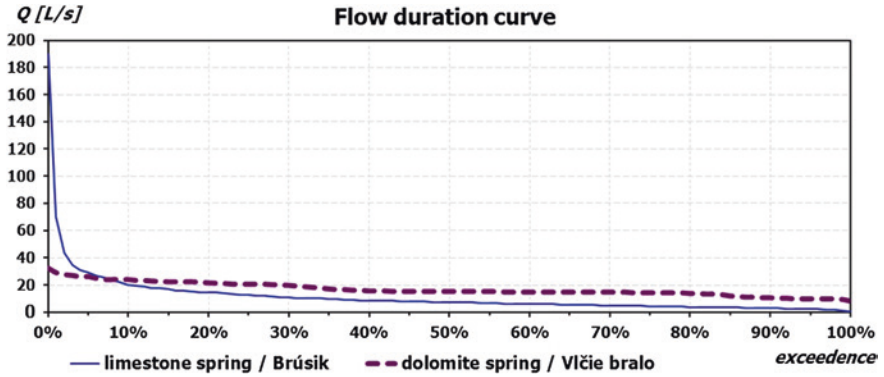

Fig. 7.5 Example of the FDC for two karstic springs—Brúsik spring dewaters pure limestones, Vlčie bralo dolomitic limestones. Discharge data are also listed in Table 7.7

It is of course better if we can construct a FDC using thousands of data points measured over many years or even decades. Here, the help of a function PERCENTILE( ) that is found in spreadsheet programs like MS Excel can be usefully exploited. Using this function, there is no need to order the discharge data according to the size (from highest to lowest). We simply reference the dataset field of all the measured discharge values («dataset») at first. We should have in mind then that we have to input the exceedence value as a residue between 1 and exceedence in a decimal format (0.7 for 30 % exceedence or 0.95 for 5 % exceedence). As an example, the PERCENTILE («dataset»; 0.8) would give the value of Q_{20} and the PERCENTILE («dataset»; 0.01) returns the value of Q_{99}.

7.4 Discharge Regime: Sub-regimes Versus Flow Components

Two simple examples of different discharge regimes shown of Fig. 7.3—the conduit-dominated karstic one and the diffuse discharge regime with much slower groundwater flow—are not only representing differences between the two groundwater circulation environments (aquifer types), but can be present within one aquifer. In traditional concept of "diffuse flow" and "quick-flow" part of discharge regime of karstic aquifers, the karst discharge regime can be composed of at least two (or more) parts recognised as sub-regimes. Complete discharge regime is then composed of superimposed sub-regimes, and majority of researchers prefer to describe these as "flow components". The two contrasting flow components typical for karst aquifers, the fast (conduit-dominated)-flow component and slow (diffuse)-flow, component are shown in Fig. 7.6. Discharge in summer and autumn period of 1979, again on Podhrad spring in Muráň, is quickly (within a day or two after precipitation) reaching the peak of several hundreds of litres per second (a tenfold discharge than the discharge before

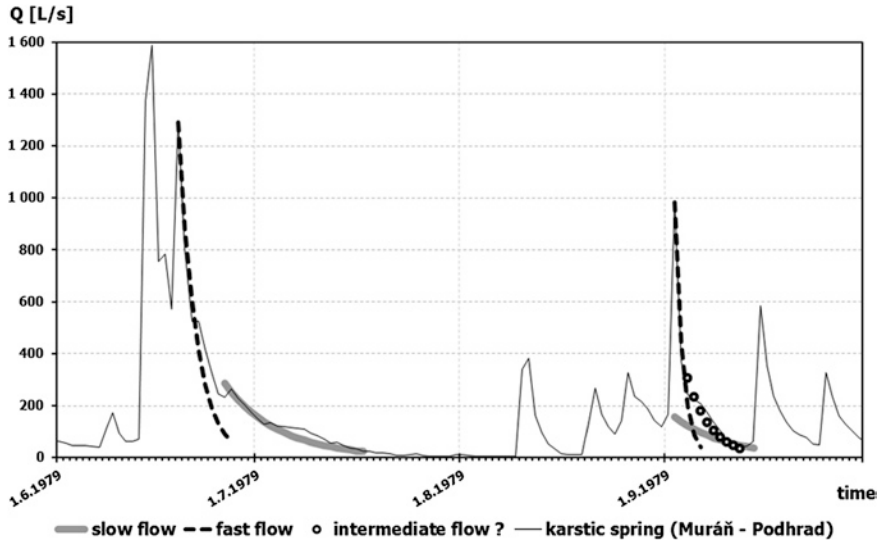

Fig. 7.6 Delineation of differently shaped sub-regimes of discharge on the recessional limb of hydrograph as different flow components—example of the Podhrad spring in Muráň municipality (Central Slovakia) during the summer period of 1979

this precipitation impulse), and then within next 4–6 days reaches the value between 100 and 200 L/s. This can be described as the quick-flow component. However, the decrease in discharge starting from the values of 100–200 L/s is not so rapid, and the discharge then reaches the previous value within the next approximately 20 days (left part of Fig. 7.6, discharge after 15 June 1979). Both fast-flow and slow-flow components here are represented by exponential function line, with different input parameters. On the right side of Fig. 7.6, however, the recessional limb of hydrograph since 2 September 1979 is different. The fast-flow component, before its complete transition to the slow-flow type of recession, is followed by another recessional type, here described as "intermediate flow". The different way of discharge declination in the period of "intermediate flow" domination, with its slope steeper than slow-flow slope and less steep than fast-flow slope, can be observed in some cases, while it is missing in other hydrologic situations. In any case, each karstic spring has a typical form of recessional hydrograph that makes it different from all other springs.

7.5 Mathematical Description of Recession and Flow Components

Boussinesq (1877) laid down the first theoretical principle of aquifer drainage and spring's discharge recession in time. His diffusion Eq. (7.5) describes flow through a porous medium:

$$\frac{\partial h}{\partial t} = \frac{K}{\varphi}\frac{\partial}{\partial x}\left(h\frac{\partial h}{\partial x}\right) \tag{7.5}$$

where

K represents hydraulic conductivity,
φ is the effective porosity (specific yield/storage coefficient) of the aquifer,
h stands for hydraulic head and
t is the time.

Using simplifying assumptions of homogeneous and isotropic intergranular unconfined aquifer of rectangular shape with concave floor, of depth H under the outlet level, where variations of h are negligible compared to aquifer depth H, neglecting capillarity effect above the water table, Boussinesq (1877) obtained an approximate analytical solution described by exponential Eq. (7.6):

$$Q_t = Q_0 \mathrm{e}^{-\alpha t} \tag{7.6}$$

where

Q_0 is the initial discharge,
Q_t is the discharge at time t and
α is the recession coefficient—an intrinsic aquifer parameter, expressed in reciprocal time units (day^{-1}) or (s^{-1}).

Maillet (1905) described similar aquifer recession curve by observations on analogous model of water-filled reservoir emptying through a porous plug—Eq. (7.6) is therefore also known as Maillet's formula. Considering the same simplifying assumptions of intrinsic aquifer properties (homogeneous, isotropic, intergranular, unconfined, rectangular shape, no capillarity), but of its shape limited by an impermeable horizontal layer at the outlet level, with curvilinear initial shape of water table (incomplete inverse beta function) where all flow velocities within the aquifer are horizontal (Dupuit–Forchheimer assumption), Boussinesq (1903, 1904) developed the analytical solution shown in Eq. (7.7):

$$Q_t = \frac{Q_0}{(1+\alpha t)^2} \tag{7.7}$$

This quadratic formula (Eq. 7.7) of discharge recession was also in accordance with results of Dewandel et al. (2003), performing numerical simulations of shallow aquifers with impermeable floor at the outlet level. Moreover, according to Boussinesq's solution (1903, 1904), physical properties of the aquifer (hydraulic conductivity K, effective porosity φ) influence values of initial discharge Q_0 and recession coefficient α parameters as shown in Eqs. (7.8) and (7.9).

$$Q_0 = 0.862Kl\frac{h_m^2}{L} \tag{7.8}$$

$$\alpha = \frac{1.115 K h_m}{\varphi L^2} \tag{7.9}$$

where

L is the width of the aquifer and
h_m is the initial hydraulic head at the distance of L,
other parameters as mentioned above.

According to Eq. (7.9), the recession coefficient α as well as initial discharge Q_0 are dependent on the initial hydraulic head h_m (in other words, on the degree of aquifer saturation). On the other hand, apart from "Maillet's exponential formula", an approximate analytical solution (linearisation) by Boussinesq (1877) has more convenient constant value of recession coefficient α. Recession coefficient here is dependent only on aquifer properties—hydraulic conductivity K, effective porosity φ, width of the aquifer L and depth of the aquifer under the outlet level H (Eq. 7.10):

$$\alpha = \frac{\pi^2 K H}{4 \varphi L^2} \tag{7.10}$$

Compared to mathematically less convenient quadratic formula (Eq. 7.7) of the Boussinesq's solution (1903, 1904), Maillet's exponential formula (Eq. 7.6; Boussinesq 1877; Maillet 1905) is widely used by hydrologists and hydrogeologists due to its simplicity and linearisation in logarithmical plots. However, various shapes of hydrograms lead many authors to formulate other recession equations, e.g. exponential reservoir model (Hall 1968) in Eq. (7.11):

$$Q_t = \frac{Q_0}{(1 + \alpha Q_0 t)} \tag{7.11}$$

Griffiths and Clausen (1997) proposed two models, one for surface water accumulations (Eq. 7.12) and one for karstic channels (Eq. 7.13)

$$Q_t = \frac{\alpha_1}{(1 + \alpha_2 t)^3} \tag{7.12}$$

$$Q_t = \alpha_1 + \alpha_2 t \tag{7.13}$$

Kullman (1990) proposed a linear model for supposed turbulent flow in conduits, analogous to discharge recession in open surface channels (Eq. 7.14), where β is the recession coefficient for quick flow (similar to linear reservoir coefficient by Bonacci (2011), or linear decrease in discharge of discharge in Torricelli reservoir by Fiorillo (2011). Kovács (2003) proposed hyperbolic model of discharge recession of karstic springs (Eq. 7.15).

$$Q_t = \left(\frac{1}{2} + \frac{|1 - \beta t|}{2(1 - \beta t)} \right) Q_0 (1 - \beta t) \tag{7.14}$$

$$Q_t = \frac{Q_0}{(1+\alpha t)^n} \tag{7.15}$$

Still, it is not easy to find the single equation that can entirely describe the recession hydrograph—this is the reason for considering participation of various subregimes (flow components) in the process of discharge recession. The first studies (starting from Maillet 1905) recognised only two basic flow components (e.g. Barnes 1939; Schöeller 1948; Werner and Sundquist 1951; Forkasiewicz and Paloc 1967; Hall 1968; Drogue 1972; Kullman 1980; Milanović 1981; Padilla et al. 1994), and later studies (e.g. Kullman 1990; Bonacci 2011; Tallaksen 1995) describe presence of more than two flow components in springs' hydrographs. In order to interpret the entire recession hydrograph, the recession limb of a karst spring hydrograph can be approximated by a function that is the sum of several exponential segments of the total recession (Eq. 7.16), or taking into account other descriptions of recession, also as Eq. (7.17) where several Kullman's Eq. (7.14) for linear discharge decrease are applied.

$$Q_t = \sum_{i=1}^{n} Q_{0i} e^{-\alpha_i t} \tag{7.16}$$

$$Q_t = \sum_{i=1}^{n} Q_{0i} e^{-\alpha_i t} + \sum_{j=1}^{m} \left(\frac{1}{2} + \frac{|1-\beta_j t|}{2(1-\beta_j t)} \right) Q_{0j}(1-\beta_j t) \tag{7.17}$$

Every *i*th or *j*th member of Eq. 7.16 or 7.17 describes one flow component, such as shown in Figs. 7.7 and 7.8.

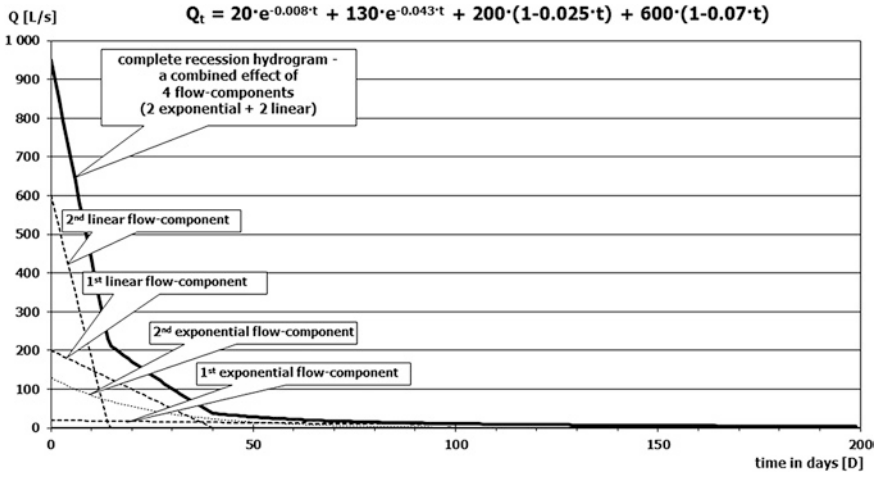

Fig. 7.7 Four flow components in ideal recession hydrograph (master recession curve)—normal plot

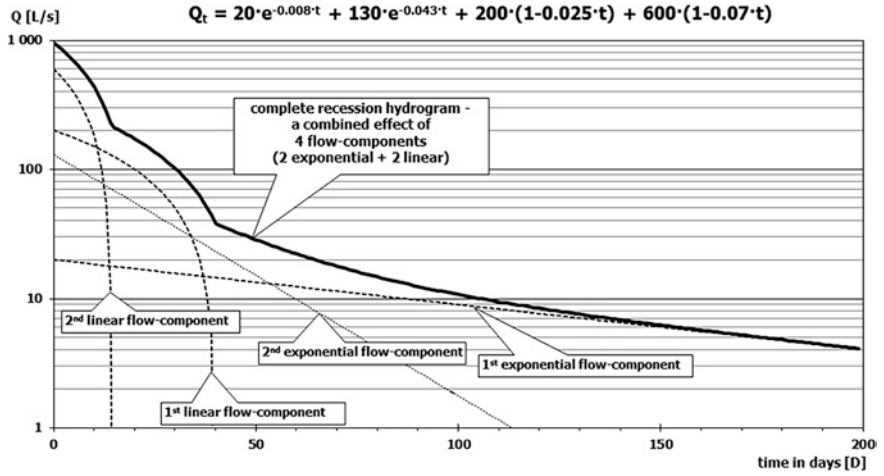

Fig. 7.8 Four flow components in ideal recession hydrograph (master recession curve)—semi-logarithmical plot

7.6 Identification of Flow Components in Recession Curves

Recession curves of karstic springs can be processed in many ways, starting from manual interpretation of the selected part of hydrograph on a paper used in matching strip method by Toebes and Strang (1964), through its digital processing (Lamb and Beven 1997; Rutlege 1998; Posavec et al. 2006; Gregor 2008) or even assembling recession discharge time series using genetic algorithms (Gregor and Malík 2012).

There are many methods for recession curve analysis, but in all of them we should select a part of the hydrograph showing the whole recessional period or its part. Evaluation of discharge threshold value, from which the recession starts (not always maximum), and the evaluation of recession period are often subjective; various authors show various criteria (Tallaksen 1995). In particular, in regions with groundwater recharge distributed within the whole hydrological cycle (e.g. moderate climate with many rainfall periods), it is not easy to distinguish the recession that is not influenced by additional recharge. The shape of recession curve is then changed—in order to avoid this problem, several methods have been developed to construct a master recession curve (MRC) from a set of shorter recessions (Tallaksen and van Lanen 2004). In this part, we should concentrate only on the analyses of the already selected recessional part of hydrograph, not taking into account whether it was assembled from several shorter recessions or selected as a single recessional event. In the hydrograph analyses, we should rely on the better visibility of linear elements by human eye and use both normal and semilogarithmical representation of the discharge time series.

The exponential flow components should be more visible in semilogarithmical graphic representation; the normal plots are more suitable for describing the linear recessional models (fast-flow components). We can also use both graph types, as shown in Fig. 7.9. The recessional part of hydrograph selected from the discharge data on Machnatá spring near Závadka and Hronom (Slovakia) is shown both in normal plot (left; Fig. 7.9a) and semilogarithmical plot (right; Fig. 7.9b). In the process of hydrograph decomposition, it is useful to start from the slow-flow (base-flow) component, which is usually of exponential nature and more visible on the semilogarithmical plot (Fig. 7.9d). This flow component is the last one that remains in the whole recessional process, and therefore, we should perform the analysis "from right to left", staring from the minimal discharge. We can derive the recession parameter of this flow component as a slope of the line that copies its shape, and starting discharge value as the discharge on the y axis that is cut by the prolongation (grey line) of this line towards the y axis showing discharge values (Fig. 7.9d). The main problem to be solved is the length of the period of basic slow-flow component domination. It should be limited by both the last and lowest discharge value on the right side, but the "left side" limitation is to be either visually estimated or computed, e.g. as the period with the best correlation coefficient of exponential regression. After the first interval was interpreted, we received the first couple of parameters: starting discharge of the first flow component Q_{01} and the recession coefficient α_1 (or β_1). In Fig. 7.9c, d, the interpreted values are 20 L/s for Q_{01} and -0.008 D^{-1} for α_1. For the next analysis step, it is better to subtract the interpreted flow component from the measured data to make the other flow components more visible (Fig. 7.9e, f). This means that from the value measured in the 48th day (here 29.83 L/s), the value $20{\cdot}e^{-0.008{\cdot}48}$ (=13.62 L/s) is subtracted giving the result of 16.20 L/s. The residual values are also shown in Fig. 7.9e, f. The interpretation then continues in the same way as in the case of the first exponential flow component (Fig. 7.9g, h), but the exponential regression (black line) and its prolongation (grey line) are described as $y = 130{\cdot}e^{-0.043x}$, and thus, $Q_{02} = 130$ L/s and $\alpha_2 = 0.043$ D^{-1}. Still, the second exponential flow component is more visible on the semilog plot (Fig. 7.9h). Figure 7.9i, j shows the recessional time series to be analysed after the next subtraction of both the first and second exponential flow components from the original values. Again, for the value measured in the 48th day (29.83 L/s), the values $20{\cdot}e^{-0.008.48}$ (=13.62 L/s) and $130{\cdot}e^{-0.043{\cdot}48}$ (=16.50 L/s) are subtracted—the result is -0.30 L/s. Similar residual values, both positive and negative, are plotted in Fig. 7.9i, j. We can see that the absolute value of these residua increases with higher discharge values showing us the uncertainties of measurement or of the chosen model. From this point, it is clear that the higher flow components are following the linear recessional model (fast-flow components). It is more convenient to interpret them on the normal plot—as in Fig. 7.9k in comparison with Fig. 7.9l. The black line of the interval analysed by linear regression and the grey line of its prolongation are described as $y = -5x + 200$ which can be in the sense of Eq. 7.14 translated into the form $y = 200(1-0.025x)$. Therefore, we interpret the parameters of the first linear flow component as $Q_{03} = 200$ L/s and $\beta_1 = 0.025$.

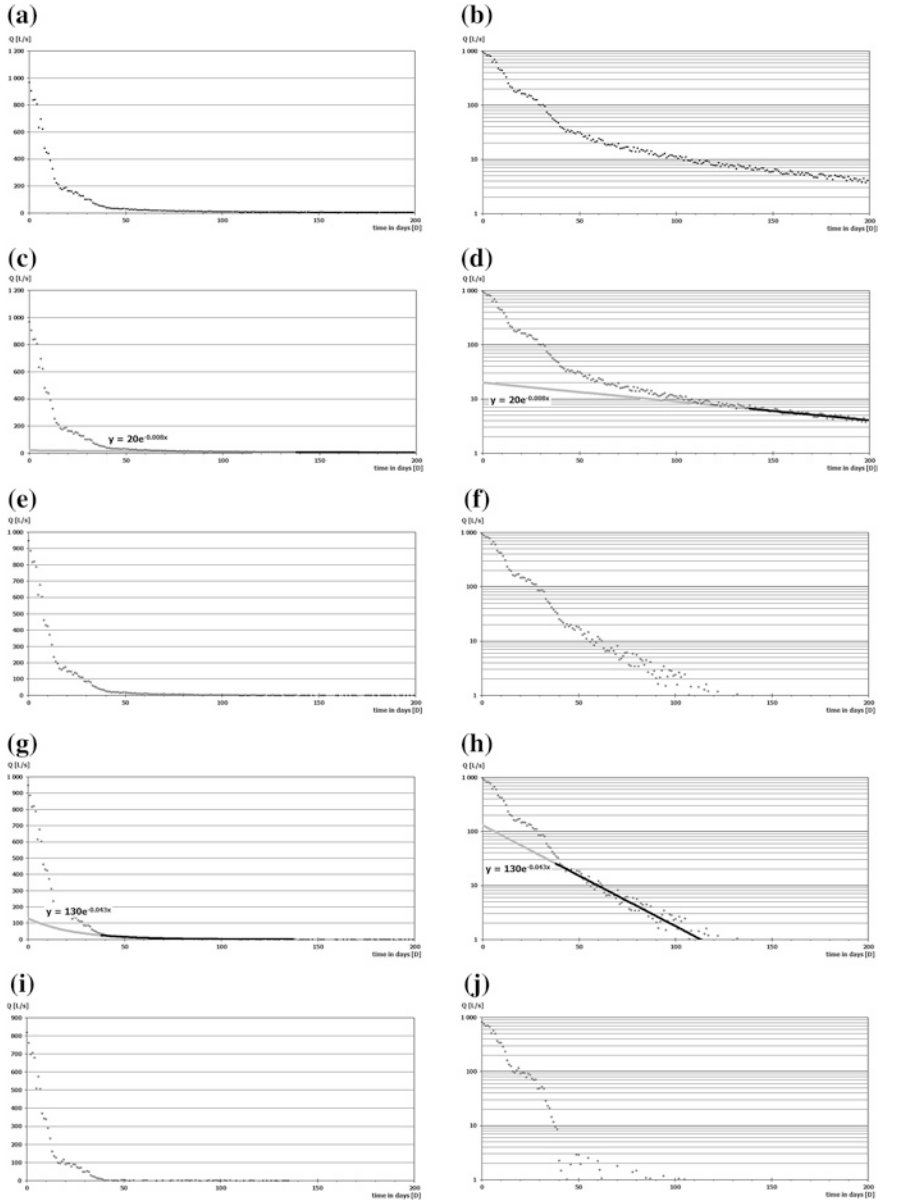
(a)
(b)
(c)
y = 20e-0.008x
(d)
y = 20e-0.008x
(e)
(f)
(g)
y = 130e-0.043x
(h)
y = 130e-0.043x
(i)
(j)
Q [L/s]
time in days [D]

Fig. 7.9 Gradual decomposition of recessional hydrograph into flow components. **a** original recessional hydrograph—normal plot; **b** original recessional hydrograph—semilog plot; **c** the first exponential flow component—normal plot; **d** the first exponential flow component—semilog plot subtraction of the first exponential flow component values—normal plot; **e** recession hydrograph after the subtraction of the first exponential flow component values—semilog plot; **f** recession hydrograph after the subtraction of the first exponential flow component values—semilog plot; **g** the second exponential flow component—normal plot; **h** the second exponential flow component—semilog plot; **i** recession hydrograph after the subtraction of the both first and second exponential flow component values—normal plot; **j** recession hydrograph after the subtraction of the both first and second exponential flow component values—semilog plot; **k** the first linear flow component—normal plot; **l** the first linear flow component—semilog plot; **m** recession hydrograph after the subtraction of the two exponential and one linear flow component values—normal plot; **n** recession hydrograph after the subtraction of the two exponential and one linear flow component values—semilog plot; **o** the second linear flow component—normal plot; **p** the second linear flow component—semilog plot; **q** the whole recession curve decomposed into four flow components (2 exponential + 2 linear; thin lines)—normal plot; and **r** the whole recession curve decomposed into four flow components (2 exponential + 2 linear; thin lines)—semilog plot

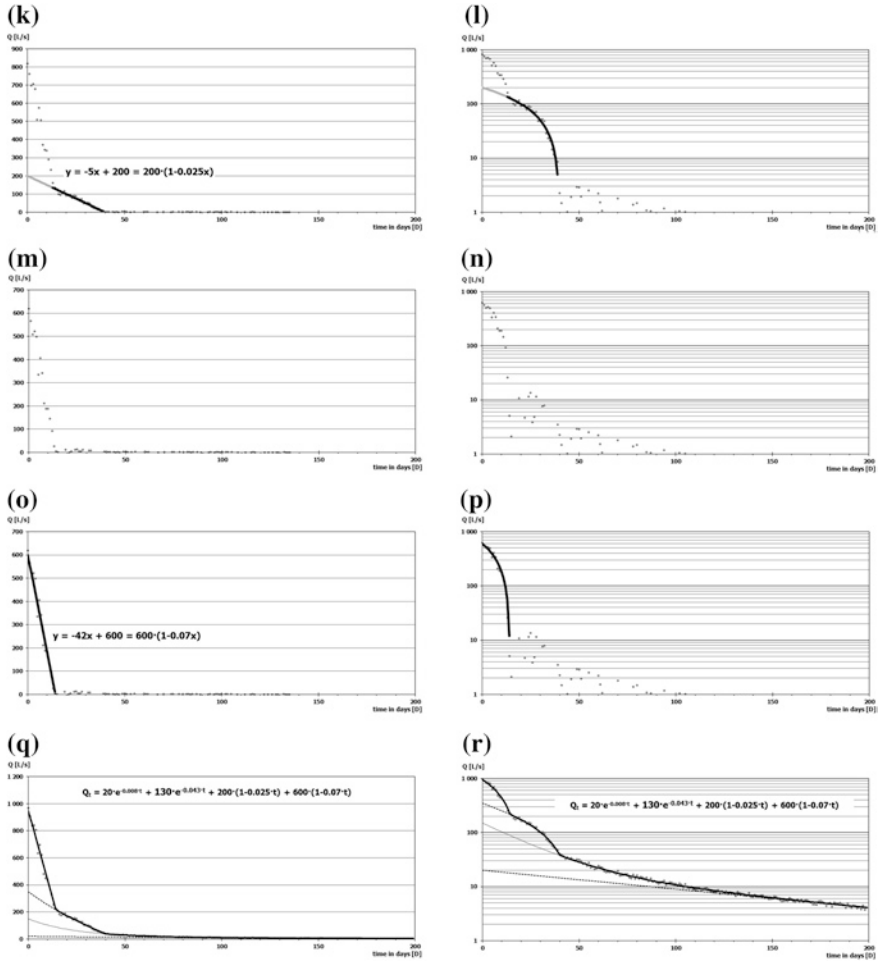

Fig. 7.9 (continued)

The values of the possible first linear flow component ought to be subtracted from the measured data together with the previous two exponential flow components, as shown in Fig. 7.9m, n. On the 7th day from the peak of 969 L/s, the measured discharge was 621 L/s. From this, 18.91 L/s belongs to the first exponential flow component ($=20{\cdot}e^{-0.008{\cdot}7}$), 96.21 L/s to the second exponential flow component ($=130{\cdot}e^{-0.043{\cdot}7}$), 165 L/s to the first linear flow component ($=200-200{\cdot}0.025{\cdot}7$), and only the rest of 341.17 L/s should be analysed. The result of this last partial recession analyses is shown in Fig. 7.9o, p described as $y = -42x + 600$, according to Eq. 7.14 translated into $y = 600(1-0.07x)$. The second linear flow component parameters are therefore $Q_{04} = 600$ L/s and $\beta_2 = 0.07$.

We should keep in mind that the duration of the exponential flow components lasts for the whole recessional period. To the left, we can prolong the interpreted duration towards the y axis ($t = 0$). To the right (higher time values), due to the nature of the exponential equation, we can still find the presence of all exponential flow components unless we set some artificial threshold value (e.g. 0.01 L/s or 1 L/s) from which we regard the presence of particular exponential flow component to be negligible. According to Eq. 7.14, the duration of each linear flow component is given by the parameter linear recession parameter β as $t_{DUR} = 1/\beta$ where t_{DUR} is the time of duration of the particular linear flow component. In the case of the recessional hydrograph shown in Fig. 7.9o, p, the first linear flow component lasts for 14 days (as $1/0.07 = 14.3$). The second linear flow component diminishes after 40 days ($1/0.025 = 40$).

There are several methods how we can place the interpretation line to the graph—in the computer, we can create a linear regression line for the part selected for interpretation or create a line input manually, having a possibility to influence its position by changed input parameters.

7.7 Calculations of Flow Component Volumes

In the sense of Eq. 7.17, we can suppose that within a complete recessional process, different volumes of particular flow components are present (Figs. 7.10 and 7.11). Total change of groundwater volume in the aquifer during the discharge recession ΔV_{exp} between the discharge Q_{t1} measured in the time t_1 and later discharge Q_{t2} measured in the time $t_2 (Q_{t1} > Q_{t2})$ can be described due to the superposition principle as the sum of volume changes within individual flow components. If the discharge recession can be described merely by one flow component (exponential Eq. 7.6), the change of groundwater volume would be as follows:

$$\Delta V_{exp} = \int_{t_1}^{t_2} Q_0 e^{-\alpha t} dt = \frac{Q_{t_1} - Q_{t_2}}{\alpha} \tag{7.18}$$

Total volume of groundwater V_{exp} that was discharged during the complete recession process within one flow component with the initial discharge of Q_0 and

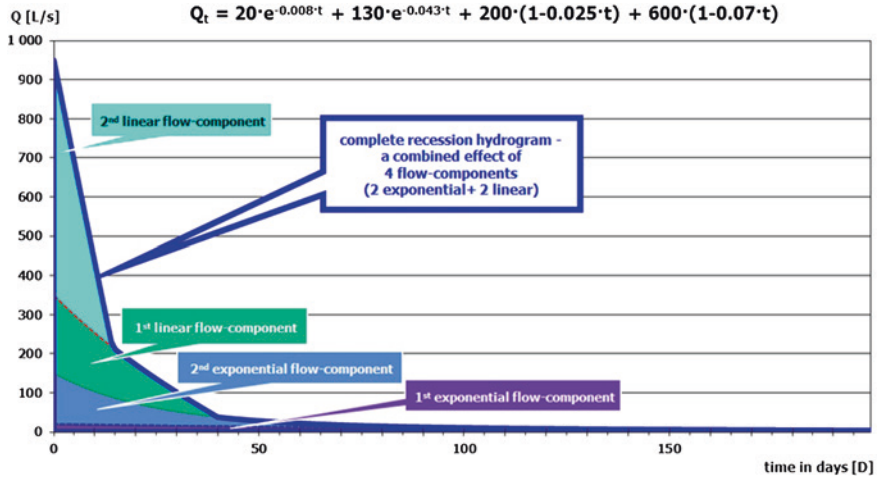

Fig. 7.10 Representation of particular volumes of flow components within a complete recessional hydrograph—normal plot

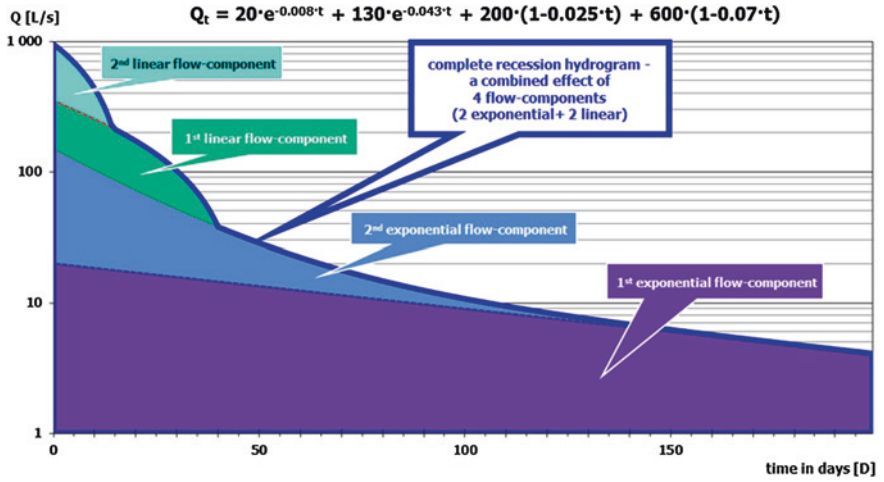

Fig. 7.11 Representation of particular volumes of flow components within a complete recessional hydrograph—semilogarithmical plot

the recession coefficient of $\boldsymbol{\alpha}$ can be then calculated as simple ratio of Q_0 and α (Eq. 7.19) as for the whole recession duration $Q_{t1} = Q_0$ and $Q_{t2} = 0$.

$$V_{\text{exp}} = \frac{Q_0}{\alpha} \tag{7.19}$$

For more (n) flow components that can be described by exponential Eq. 7.6, the total groundwater volume change ΔV_{exp} between the discharge Q_{t1} measured in the time t_1 and discharge Q_{t2} measured in the time t_2 ($t_2 > t_1$ and $Q_{t1} > Q_{t2}$) is the summation of volume changes in all flow components (Eq. 7.20).

$$\Delta V_{\text{exp}} = \sum_{1}^{n} \int_{t_1}^{t_2} Q_0 \mathrm{e}^{-\alpha t} \mathrm{d}t = \frac{Q_{1t_1} - Q_{1t_2}}{\alpha_1} + \cdots + \frac{Q_{nt_1} - Q_{nt_2}}{\alpha_n} \tag{7.20}$$

While performing aforementioned calculations, one should have in mind the correct use of units: recession coefficients are usually in units (day^{-1}) and discharges in (L s^{-1}), so if we want to know the volume change in cubic metres (m^3), we have to convert discharges into (m^3 day^{-1}) or (m^3 s^{-1}), but in the second case we need also the conversion of recession coefficients from (day^{-1}) into (s^{-1}).

Change of groundwater volume in linear recession model (Eq. 7.14) ΔV_{lin} in the similar solution, where β is the linear recession coefficient, can be for one linear sub-regime described as in Eq. 7.21. The discharge Q_{t1} corresponds to the time t_1 and discharge Q_{t2} to the time t_2; $t_2 > t_1$ and $Q_{t1} > Q_{t2}$; both time t_1 and time t_2 are fulfilling the condition of being $< 1/\beta$ to obtain only positive Q_{t1} and Q_{t2} values. The whole volume discharged in each individual flow component of linear recession model (where $Q_{t1} = Q_0$ and $Q_{t2} = 0$) can be calculated according to Eq. 7.22.

$$\Delta V_{\text{lin}} = \int_{t_1}^{t_2} Q_0 (1 - \beta t) \mathrm{d}t = \frac{Q_{t_1}^2 - Q_{t_2}^2}{2 Q_0 \beta} \tag{7.21}$$

$$V_{\text{lin}} = \frac{Q_0}{2\beta} \tag{7.22}$$

For several quick-flow components (m) described by linear Eq. 7.14, the groundwater volume change ΔV_{lin} discharged (usually quick-flow components) between the moment of time t_1 and t_2 can be calculated as shown in Eq. 7.23.

$$\Delta V_{\text{lin}} = \sum_{1}^{m} \int_{t_1}^{t_2} Q_0 (1 - \beta_m t) \mathrm{d}t = \frac{Q_{1t_1}^2 - Q_{1t_2}^2}{2 Q_{01} \beta_1} + \cdots + \frac{Q_{mt_1}^2 - Q_{mt_2}^2}{2 Q_{0m} \beta_m} \tag{7.23}$$

Also here, using Eqs. 7.22 and 7.23, we should be careful about the units, as β is usually given in (D^{-1}) and Q in L/s or m^3/s so we should express β in (s^{-1}) by dividing it by the number of seconds within a day (86,400). If both linear flow components and exponential flow components were identified in the discharge recession process, calculation of the total change of groundwater volume in the aquifer ΔV is as in Eq. 7.24.

$$\Delta V = \sum_{1}^{n} \int_{t_1}^{t_2} Q_0 \mathrm{e}^{-\alpha t} \mathrm{d}t + \sum_{1}^{m} \int_{t_1}^{t_2} Q_0 (1 - \beta_m t) \mathrm{d}t \tag{7.24}$$

and then

$$\Delta V = \frac{Q_{1t_1} - Q_{1t_2}}{\alpha_1} + \cdots + \frac{Q_{nt_1} - Q_{nt_2}}{\alpha_n} + \frac{Q_{1t_1}^2 - Q_{1t_2}^2}{2Q_{01}\beta_1} + \cdots + \frac{Q_{mt_1}^2 - Q_{mt_2}^2}{2Q_{0m}\beta_m}$$

7.8 Hydrograph Separation into Flow Components

Hydrograph separation into flow components is a tool for distinguishing basic proportions of individual flow components present in total discharge. It enables quantitative referencing of flow components for further interpretations, e.g. for the purposes of estimation of the quick-flow duration or securing the exploitable amounts of karstic groundwater for longer periods. Or, at least, by the help of hydrograph separation, the diminishing points (in time) of individual flow components can be defined and proportions of individual flow components present at every stage of discharge can be quantified.

Hydrograph separation can be performed manually, by creation of stencil that is step by step laid directly to the hydrograph, while the lines of the respective flow component are gradually depicted on the same paper. The same process can be similarly performed by creation of MRC using the set of equations and input parameters that enable creation of virtual replica of MRC. The main idea behind this method is based on a simplified understanding of a hydrologic system reality: the same discharge should reflect the same water saturation (piezometric) level in the system. Although this assumption is a gross simplification, this method still may be helpful in quantitative referencing of flow components for further interpretations. In reality, temporary unequal distribution of saturation levels is usual in quantitative behaviour of karstic aquifers. Within karstified rock masses, several piezometric levels should exist at least for each saturated system (small fissures, medium fissures, karst conduits), if not for their different parts. Time dependency of these individual piezometric levels then substantially differs one from another. In spite of all, facing practical problems, the discharge data are in most cases the only values that may provide quantitative reference describing the whole system.

Principles of hydrograph separation based on master recession are demonstrated in Fig. 7.12. On the left side of Fig. 7.12, there is a typical MRC (violet line) delineated by superposition of 3 flow components—2 exponential and one linear. On the right side of Fig. 7.12, there is a part of real discharge hydrograph measured on the same spring. Individual flow components on the left side are highlighted by different patterns. Two horizontal lines starting on points Q_a and Q_b at the real discharge hydrograph from the right side of Fig. 7.12 are intersecting the MRC at corresponding two discharge levels of Q_A and Q_B. Each of these two discharges (Q_A and Q_B) on MRC is composed of different proportional representation of flow components, as visible on vertical bars drawn down from the intersections. In the case of the discharge Q_A, 3 flow components are present, while only

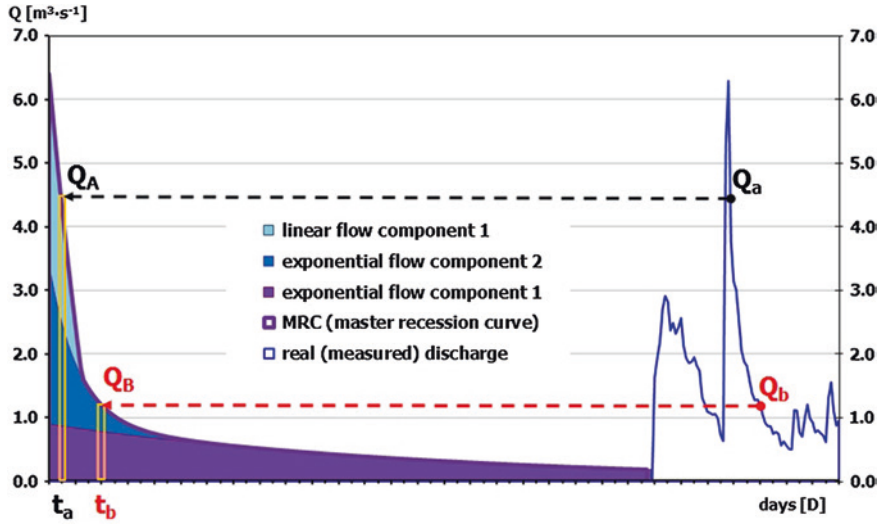

Fig. 7.12 Principles of hydrograph separation into flow components using master recession curve parameters

two flow components are found to sum up the discharge Q_B. This is to demonstrate that for every discharge on the right side of the figure, relevant value on recession curve is found (by calculation, as described later). Figure 7.12 also shows that each measured discharge value can be divided into several sub-regimes, depending on its position on the MRC. Also, every discharge value can be described by representative time t_R that had theoretically elapsed from the maximum discharge value $Q_{\max}$: discharge Q_A by the time t_a and discharge of Q_B by the time t_b as described in the following text.

Every karstic spring can be described by its own MRC, or—in other words—by unique set of parameters, individual constant values of starting discharges $Q_{01} \ldots Q_{0n}$ and $Q_{01} \ldots Q_{0m}$ and recession coefficients ($\alpha_1 \ldots \alpha_n$ and perhaps $\beta_1 \ldots \beta_m$). These parameters should be determined for each detected flow component (sub-regime). Theoretically, every equation from the aforementioned set of recession Eqs. (7.6, 7.7, 7.11–7.14 or 7.15) or also other recession equations can be applied—here, it is sufficient to use Eqs. 7.6 and 7.14.

In the process of hydrograph separation into individual flow components, each measured discharge value is understood to be composed of at least one flow component or superposition of two or more flow components. In the following text, several slow-flow components (exponential recession) and eventually also quick-flow components expressed by linear recession model are considered. According to Eq. 7.17, every measured discharge value Q_t is determined merely by ***representative time*** t_R, i.e. time that had theoretically elapsed from the absolute (overall) maximum discharge value $Q_{\max}$. This means that every discharge can be written just by substitution of the representative time t_R into Eq. 7.17. Subsequently,

using the representative time t_R substituted into partial flow component equations, amounts discharged in these flow components can be calculated. For every flow component of exponential recession model, the representative time t_R can be calculated according to Eq. 7.25:

$$t_R = \frac{\ln Q_t - \ln Q_0}{-\alpha} \tag{7.25}$$

and for time t fulfilling the condition $t < 1/\beta$, the representative time t_R of (fast-flow) linear model flow components can be calculated according to Eq. 7.26

$$t_R = \frac{1}{\beta}\left(1 - \frac{Q_t}{Q_0}\right) \tag{7.26}$$

Having in mind that the karst spring recession hydrograph can be composed by summation of several exponential segments and several linear segments (Eq. 7.17), it is convenient to perform the computation of each theoretically elapsed time t_R by iteration process. Iterative method is a mathematical procedure that generates a sequence of improving approximate solutions up to some termination criteria which here, discussing the discharge of springs, can be related to the accuracy of discharge measurement. In practice, 10 iteration procedures were usually sufficient to give result within the discharge reading accuracy. Iterative solution is based on comparison of two solutions influencing the next iteration step (procedure). It is convenient to set the two starting t_R time inputs as $t_{R1} = 0$ (minimum value) and $t_{R2} = 1/\alpha_1$ (maximum value). In the next iteration step, the value of t_R achieved in the previous solution is substituted into Eq. 7.17 and the result is compared to the measured discharge Q_t. If it is higher, half of the interval between the two previous t_R values is added to the t_R in next iterative solution step. If the substituted Q_t value is lower than measured, the t_R in the next solution is lowered in one half of the interval between the two previous calculations of t_R values. In the next iteration step again, if after the substitution the Q_t value is lower than real, the proposed t_R value in the next solution is lower in one half of the interval between the two previous calculations of t_R values and vice versa. Gradual development of iterative solutions is repeatedly compared to the measured value and can be arbitrarily stopped if the difference is negligible enough, or—as stated before—is set to stop perhaps after the 10th or 20th iteration procedure. As the sequence of Eqs. 7.17 converges for given initial approximations, this iterative method is convergent.

In this way, for each measured discharge value Q_t, we can calculate the representative time t_R that enables its decomposition into flow components. Eq. 7.17 suggests that there are periods, when all flow components are present in the spring's discharge, and also periods when they gradually, one after another, diminish. In Eq. 7.17, all flow components are sufficiently described by their partial starting (maximal) discharges $Q_{0n} \ldots Q_{0m}$ and recession coefficients $\alpha_n \ldots \beta_m$. We should note that the representative time t_R that had theoretically elapsed from the maximal discharge Q_{max} is the same for each flow component. We can receive the actual partial discharge for each of the flow components (sub-regimes) by

substitution of the t_R to its partial Eq. 7.6 or 7.14, but also other recession equations, e.g. Eqs. 7.7, 7.11–7.13 or 7.15. To check the calculation, the total discharge Q_t has to be the sum of these partial discharges.

Knowing the representative time t_R for each discharge value, proportional amounts of different discharging flow components can be calculated in one moment (Fig. 7.12), or for the whole evaluated period (Figs. 7.10 and 7.11). Presence of individual flow components can be expressed in discharge units (in L/s or m^3/s) for one moment of spring's discharge or as average discharges (average discharge of slow-flow component, etc.). The MRC shown in Fig. 7.12 can be described by Eq. 7.27. Discharge units here are m^3/s.

$$Q_t = 0.9e^{-0.007t} + 2.5e^{-0.09t} + 3.0(1 - 0.08t) \tag{7.27}$$

Another way of presentation of the results of hydrograph decomposition is to show the flow components in volumes discharged within the duration of evaluated periods. For example, the discharge $Q_a = Q_A$ of 4,661 L/s in Fig. 7.12 according to Eq. 7.27 consists of the slow-flow discharge of 875 L/s, "another slow-flow" component (exponential flow component 2) of 1,744 L/s (flow component with higher recession coefficient α) and the quick-flow component of 2,040 L/s. During the complete recession process in Fig. 7.12, using Eqs. 7.19 and 7.22, the volume of 11,108,571 m^3 was discharged within the slow-flow component, next 2,400,000 m^3 was discharged within the flow component with higher recession coefficient, and 1,620,000 m^3 was discharged as quick-flow component. The total volume of water discharged during the whole recession is then 15,128,571 m^3.

The advantage of the use of MRC parameter's hydrograph separation method is the clear solution for every discharge value it allows. However, described understanding of underground hydrologic system functions (assumption that the same discharge reflects the same water saturation or piezometric level in the aquifer) is a gross simplification. In reality, temporary unequal distribution of saturation levels is usual in aquifer's quantitative behaviour. Within karstic aquifers, several piezometric levels should exist at least for each saturated system (small fissures, medium fissures, karst conduits), if not for their different parts. Time dependency of these individual piezometric levels then substantially differs one from another. Király (2003) and Kovács et al. (2005) described recession coefficient as a global parameter depending on global configuration of the karst aquifers (also form and extension) and do not recommend its use to for aquifer hydraulic properties calculations. The same author underlines the role of mixing processes and dilution within the aquifer and shows that improperly used chemical or isotopic hydrograph separation methods may lead to invalid inferences regarding the groundwater flow processes. In spite of all, facing practical problems, the discharge values are in most cases the only data that represent quantitative reference describing the whole system. Simplified hydrograph separation method, based on proper recession curves analyses of the whole discharge time series in such cases, can help to distinguish and quantitatively express basic proportions of individual flow components. The aforementioned method is at least useful as quantitative reference of flow components for further interpretations. Also, by its help, the diminishing or

starting point of individual flow components can be properly quantified, such as knowledge that the quick-flow component often connected with unwanted turbidities in the water source diminishes within 12.5 days after the peak maximum discharge (Eq. 7.27, Fig. 7.12), which might be useful from the water management point of view.

Case study 1. Assessment of spring discharge variability

Dolné Veterné is a spring far away from the inhabited areas of the Veľká Fatra Mts. (Slovakia). It was not possible to perform regular observations of its discharge more frequently than once a month. Within a year period, the observer provided discharge measurement results as follows (Figs. 7.13 and 7.14).
Try to apply classification criteria as degree of spring's reliability, degree of spring's discharge stability, SVC, degree of spring's discharge stability and SCVP *on the Dolné Veterné spring.*

Date	Q—discharge in L/s
07.11.2001	11.00
05.12.2001	17.20
02.01.2002	14.00
06.02.2002	27.70
06.03.2002	36.40
03.04.2002	33.20
01.05.2002	30.10
05.06.2002	25.30
03.07.2002	17.20
07.08.2002	13.20
04.09.2002	16.00
02.10.2002	15.60

Fig. 7.13 Spring Dolné Veterné in Gaderská dolina valley (Blatnica municipality) in the second decade of the twenty-first century—photograph from the database of the Slovak Hydrometeorological Institute

Exercise
Using the twelve discharge data above, we receive

$Q_{min} = 11.00$ L/S (Eq. 7.1)
$Q_{max} = 36.40$ L/S (Eq. 7.1)
$\Phi = 21.41$ L/S (Eq. 7.2)
$Q_{10} = 32.89$ L/S (Eq. 7.3)
$Q_{90} = 13.28$ L/S (Eq. 7.3)
$\sigma = 8.65$ L/S (Eq. 7.4)

Solution
By using Eq. (7.1), the value of variability index I_v is 3.31—according to this, degree of spring's reliability (Table 7.2) is *very good*. According to Table 7.3, degree of spring's discharge stability is *unstable*.
Equation (7.2) gives value of spring variability *V* as 119 %, and the spring should be supposed as *variable*.
SVC according to Eq. (7.3) equals 2.48, and its classification using this coefficient should be "*steady*" (Table 7.4), or the degree of spring's discharge stability can be described as "*very stable*" (Table 7.5).
According to Eq. (7.4), the value of SCVP is 0.40. Its variability is then classified as "*low*" (Table 7.6).

P.S.: From this spring (Dolné Veterné), weekly discharge data were taken for a period of more than 30 years since 1978; for preparation of this exercise, only few of them were selected. Based on the 1357 readings of weekly gauging results for the period 1978–2004, the complete dataset would give results as $Q_{min} = 3.16$ *L/s;* $Q_{max} = 82.40$ *L/s;* $\Phi = 21.46$ *L/s;* $Q_{10} = 34.20$ *L/s;* $Q_{90} = 8.93$ *L/s; and* $\sigma = 9.83$ *L/s. The spring would then reach bad reliability* (Table 7.2) *and very unstable discharge stability* (Table 7.3) *as variability index* $I_v = 26.08$*; but according to* Table 7.4 *would be well balanced and stable* (Table 7.5) *as SVC = 3.83; with low SCVP* (Table 7.6*; SCVP = 0.46*), *while V = 369 %* (Eq. 7.2). *This is to illustrate the importance of discharge gauging time span.*

Case study 2. Construction of FDC duration curve, calculation of exceedence

Try to calculate discharge exceedence Q_1*;* Q_5*;* Q_{10}*;* Q_{20}*;* Q_{30}*;* Q_{40}*;* Q_{50}*;* Q_{60}*;* Q_{70}*;* Q_{80}*;* Q_{90}*;* Q_{95}*; and* Q_{99} *using the data from the Dolné Veterné spring in the Case study 1. The dataset here is quite limited, but using the PERCENTILE () function in MS Excel, you will be able to cope with the task. Based on the exceedence data, draw a graph of the FDC.*

Exercise
In MS Excel, use the function PERCENTILE («dataset» ;«percentage») with references to «dataset» as «A2:A13» and «percentage» derived from column «C» as follows:

	A	B	C	D
1	*Q* (L/s)		%	Q_x
2	11.00		1	=PERCENTILE(A2:A13;1-C2)
3	17.20		5	=PERCENTILE(A2:A13;1-C3)
4	14.00		10	=PERCENTILE(A2:A13;1-C4)

	A	B	C	D
5	27.70		20	=PERCENTILE(A2:A13;1-C5)
6	36.40		30	=PERCENTILE(A2:A13;1-C6)
7	33.20		40	=PERCENTILE(A2:A13;1-C7)
8	30.10		50	=PERCENTILE(A2:A13;1-C8)
9	25.30		60	=PERCENTILE(A2:A13;1-C9)
10	17.20		70	=PERCENTILE(A2:A13;1-C10)
11	13.20		80	=PERCENTILE(A2:A13;1-C11)
12	16.00		90	=PERCENTILE(A2:A13;1-C12)
13	15.60		95	=PERCENTILE(A2:A13;1-C13)
14			99	=PERCENTILE(A2:A13;1-C14)

Solution

We can derive following exceedence values from the data given in the Case study 1 (also in the A2:A13 database above):

Q_1	Q_5	Q_{10}	Q_{20}	Q_{30}	Q_{40}	Q_{50}	Q_{60}	Q_{70}	Q_{80}	Q_{90}	Q_{95}	Q_{99}
36.05	34.64	32.89	29.62	26.98	22.06	17.20	16.48	15.72	14.32	13.28	12.21	11.24

From these, we can plot a FDC like this (in thick line, data from the table above are used).

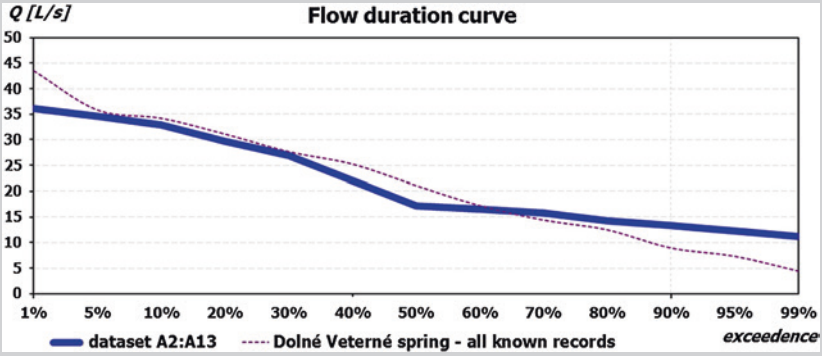

Fig. 7.14 Flow duration curve—spring Dolné Veterné in Gaderská dolina valley (Blatnica municipality); *thick line* is for the exercise dataset A2:A13; *scattered thin line* is derived from all known discharge records (1,357 records taken weekly): note that the curves differ mainly at the beginning (*maximal values*) and the end (*minimal values*) of the lines

Case study 3. Plotting of theoretical recession curve, calculation of flow component volumes and duration of flow components

For spring XY, after recession curve analyses, MRC was created with two exponential flow components (following Eq. 7.6*) and two linear flow components (following* Eq. 7.14*). Following parameters were identified for*

individual flow components: $Q_{01} = 58.7$ *L/s and* $\alpha_1 = 0.005\ D^{-1}$ *for the first exponential flow component and* $Q_{02} = 174.9$ *L/s and* $\alpha_2 = 0.08\ D^{-1}$ *for the second exponential flow component. For the two flow components following linear depletion model* (Eq. 7.14), $Q_{03} = 629$ *L/s and* $\beta_1 = 0.04\ D^{-1}$ *were for the first and* $Q_{04} = 2450$ *L/s and* $\beta_2 = 0.3\ D^{-1}$ *for the second linear flow component. Try to calculate decrease in individual flow components using* Eqs. 7.6 *and* 7.14*, as well as to find values for the whole recessional process.*

Exercise

In MS Excel, use the EXP ( ) function for the first two "slow-flow" components. Input parameters in the following table are marked as bold and shaded. Calculate values of the flow components up to 160 days after the maximum. Then, plot the data of both flow components into one graph with normal plot of discharge values on another graph with logarithmical *y* axis for discharge. Try to play with the input data in the fields $B$1, $B$2, $B$6 and $B$7 (make recession coefficients or starting discharges bigger or smaller), and see how the plotted curves change their shape.

	A	B	C	D	E	F
1	**alpha1 [1/D]**	**0.005**		**time [days]**	**exponential 1**	**exponential 2**
2	**alpha2 [1/D]**	**0.08**		0	=$B$6*EXP(-$B$1*$D2)	=$B$7*EXP(-$B$2*$D2)
3	**beta1 [1/D]**	**0.04**		1	=$B$6*EXP(-$B$1*$D3)	=$B$7*EXP(-$B$2*$D3)
4	**beta2 [1/D]**	**0.3**		2	=$B$6*EXP(-$B$1*$D4)	=$B$7*EXP(-$B$2*$D4)
5				3	=$B$6*EXP(-$B$1*$D5)	=$B$7*EXP(-$B$2*$D5)
6	**Q01 [L/s]**	**58.7**		4	=$B$6*EXP(-$B$1*$D6)	=$B$7*EXP(-$B$2*$D6)
7	**Q02 [L/s]**	**174.9**		5	=$B$6*EXP(-$B$1*$D7)	=$B$7*EXP(-$B$2*$D7)
8	**Q03 [L/s]**	**629**		6	=$B$6*EXP(-$B$1*$D8)	=$B$7*EXP(-$B$2*$D8)
9	**Q04 [L/s]**	**2450**		7	=$B$6*EXP(-$B$1*$D9)	=$B$7*EXP(-$B$2*$D9)
10				8	=$B$6*EXP(-$B$1*$D10)	=$B$7*EXP(-$B$2*$D10)
…				...	…	…
160				158	=$B$6*EXP(-$B$1*$D160)	=$B$7*EXP(-$B$2*$D160)
161				159	=$B$6*EXP(-$B$1*$D161)	=$B$7*EXP(-$B$2*$D161)
162				160	=$B$6*EXP(-$B$1*$D162)	=$B$7*EXP(-$B$2*$D162)

For the linear flow components, use another expression but the same input parameters:

	A	B	C	D	...	G	H
1	**alpha1 [1/D]**	**0.005**		**time [days]**	...	**linear 1**	**linear 2**
2	**alpha2 [1/D]**	**0.08**		0	...	=IF($B$8*(1-$B$3*$D2)<0;0;$B$8*(1-$B$3*$D2))	=IF($B$9*(1-$B$4*$D2)<0;0;$B$9*(1-$B$4*$D2))
3	**beta1 [1/D]**	**0.04**		1	...	=IF($B$8*(1-$B$3*$D3)<0;0;$B$8*(1-$B$3*$D3))	=IF($B$9*(1-$B$4*$D3)<0;0;$B$9*(1-$B$4*$D3))
4	**beta2 [1/D]**	**0.3**		2	...	…	…
5				3	...	…	…
6	**Q01 [L/s]**	**58.7**		4	...	…	…
7	**Q02 [L/s]**	**174.9**		5	...	…	…
8	**Q03 [L/s]**	**629**		6	...	…	…
9	**Q04 [L/s]**	**2450**		7	...	…	…
…				...	...	…	…
161				159	...	=IF($B$8*(1-$B$3*$D161)<0;0;$B$8*(1-$B$3*$D161))	=IF($B$9*(1-$B$4*$D161)<0;0;$B$9*(1-$B$4*$D161))
162				160	...	=IF($B$8*(1-$B$3*$D162)<0;0;$B$8*(1-$B$3*$D162))	=IF($B$9*(1-$B$4*$D162)<0;0;$B$9*(1-$B$4*$D162))

In the linear flow components, their values would quickly fall below zero—to eliminate the influence of the negative values on the final result, the simple formula = $B$8*(1−$B$3*$D2) for the cell G2 has to be blocked out for values bellow zero. In Eq. 7.14, the part of the formula $\left(\frac{1}{2} + \frac{|1-\beta t|}{2(1-\beta t)}\right)$ serves the same purpose, but in spreadsheet we can do it manually—e.g. by formulae = IF($B$8*(1-$B$3*$D2) < 0;0;$B$8*(1-$B$3*$D2)) for the cell G2 and so on.

Add the data of both linear flow components into the previous graphs (normal and semilog one). Try to change the input data in the fields $B$3, $B$4, $B$8 and $B$9 (make them bigger or smaller), and see how the plotted curves change their shape.

For creating the whole MRC, do the sum of all partial flow components: count together columns «E» + «F» + «G» + «H». Try to change the

input data in the fields $B$1–$B$4 and $B$6–$B$9 (make them bigger or smaller), and see how the main plotted (MRC) and the recession curves of partial flow components change the shape with different combination of input values both in normal and semilogarithmical plot.

Exercise

Now, having the recession described by Eq. (7.28)*, we should try to calculate volumes of individual flow components that are depleted within the whole recessional process.*

$$Q_t = 58.7\mathrm{e}^{-0.005t} + 174.9\mathrm{e}^{-0.08t} + 629(1 - 0.04t) + 2450(1 - 0.3t) \qquad (7.28)$$

Solution

Volume of water discharged within individual flow components is illustrated as an area of different colour, delineated by axes and curves or lines of flow component functions of Figs. 7.10 and 7.11. For exponential flow, Eq. 7.19 and for linear model flow component, Eq. 7.22 are used for calculation of the whole volume discharged within the complete recession cycle. Summation of partial volumes of individual flow components also represents the maximal water storage within the dewatered aquifer or within the recharge area. Partial volumes can be linked to storage in small or bigger fissures (slow-flow/exponential components) or conduits and karst channels (quick-flow/linear model components).

$$V_{\mathrm{exp1}} = \frac{Q_{01}}{\alpha_1} = \frac{58.7/1{,}000}{0.005/86{,}400} = 1{,}014{,}336\,\mathrm{m}^3$$

$$V_{\mathrm{exp2}} = \frac{Q_{02}}{\alpha_2} = \frac{174.9/1{,}000}{0.08/86{,}400} = 188{,}892\,\mathrm{m}^3$$

V_{exp1} is the volume discharged within the first exponential flow component, V_{exp2} within the second one. Note that number of 86,400 s within a day was used in the denominator, as the recession coefficients were in the (D^{-1}) units. Also, divided by 1,000, discharge in the numerator was recalculated from (L/s) units into (m^3/s) units. We can see here that although starting discharge of the second exponential flow component is three times bigger than that of the first one, due to small recession coefficient, the water volume discharged in first exponential flow component in more than five times prevails over the second one. From this, we can also judge on the volume of joints and fissures with different apertures.

$$V_{\mathrm{lin1}} = \frac{Q_{03}}{2\beta_1} = \frac{629.0/1{,}000}{2 \cdot 0.04/86400} = 679{,}320\,\mathrm{m}^3$$

$$V_{\text{lin2}} = \frac{Q_{04}}{2\beta_2} = \frac{2{,}450.0/1000}{2 \cdot 0.3/86{,}400} = 352{,}800\,\text{m}^3$$

Volume discharged in the first quick-flow (linear) component V_{lin1} is nearly two times as big as in the second case (V_{lin2}). Recalculation for units (from (L/s) to (m^3/s) and from (D^{-1}) to (s^{-1})) is applied also here. The total discharged volume is then

$$\begin{aligned} V_{\text{TOTAL}} &= \frac{Q_{01}}{\alpha_1} + \frac{Q_{02}}{\alpha_2} + \frac{Q_{03}}{2\beta_1} + \frac{Q_{04}}{2\beta_2} \\ &= \frac{58.7/1000}{0.005/86400} + \frac{174.9/1000}{0.08/86400} + \frac{629.0/1{,}000}{2 \cdot 0.04/86{,}400} \\ &\quad + \frac{2{,}450.0/1{,}000}{2 \cdot 0.3/86{,}400} \\ &= 2{,}235{,}348\,m^3 \end{aligned}$$

Exercise

Try to calculate volume of water discharged within the first exponential flow component during the period while its partial discharge decreased from 40 to 30 L/s. For the second linear flow component, try to calculate volume of water discharged within this particular sub-regime while it had fallen down from 2,000 to 1,000 L/s. Apply on the same spring described by the same recessional Eq. (7.28).

Solution

The change of groundwater volume discharged within single recessional flow component of exponential nature (Eq. 7.6) between two given discharge values is described by Eq. 7.18. In our case, $Q_{t1} = 40.0$ L/s and $Q_{t2} = 30.0$ L/s. Then, using Eq. 7.18,

$$\Delta V_{\text{exp}} = \frac{Q_{t_1} - Q_{t_2}}{\alpha} = \frac{40/1{,}000 - 30/1{,}000}{0.005/86{,}400} = 172{,}800\ \text{m}^3$$

Again, note that L/s had to be converted into (m^3/s) and (D^{-1}) into (s^{-1}) to receive the result in (m^3).

Equation 7.21 is used to calculate the change of groundwater volume in linear recession model; in our task, the discharge in time t_1 was $Q_{t1} = 2{,}000.0$ L/s and Q_{t2} in time t_2 was 1,000.0 L/s. The partial starting discharge for the second linear flow component (see it in Eq. 7.28) $Q_{04} = 2{,}450.0$ L/s. Also here, we have to take care about the units. Then,

$$\Delta V_{\text{lin}} = \frac{Q_{t_1}^2 - Q_{t_2}^2}{2Q_0\beta} = \frac{(2{,}000/1{,}000)^2 - (1{,}000/1{,}000)^2}{2 \cdot (2{,}450/1{,}000) \cdot (0.3/86{,}400)} = 58{,}776\ \text{m}^3$$

We can see that although discharges within the second linear flow component are enormous in comparison with those we have in the first exponential

flow component, the total volume discharged in the slow-flow component while it drops from 40 to 30 L/s is nearly 3 times as big as discharged within quick flow.

Exercise
Try to calculate duration of individual flow components, both exponential and linear, having the same recession described by Eq. (7.28).

Solution
Duration of each linear model flow component can be described by Eq. 7.26; we should just assume that it is the moment when Q_t reaches zero. For the first linear flow component, then,

$$t_{\mathrm{DUR-linear1}} = \frac{1}{\beta_1}\left(1 - \frac{Q_t}{Q_{03}}\right) = \frac{1}{0.04}\left(1 - \frac{0}{Q_{03}}\right) = \frac{1}{0.01} = 25 \text{ days}$$

Note that there is no recalculation from (D^{-1}) unit of the recession coefficient into (s^{-1}), and therefore, the result is expressed in days. For the second linear flow component, then, the time of its duration $t_{\mathrm{DUR-linear2}}$ is calculated as

$$t_{\mathrm{DUR-linear2}} = \frac{1}{\beta_2} = \frac{1}{0.3} = 3.3 \text{ days}$$

The exponential formula used for the slow-flow description (Eq. 7.6) causes that each slow-flow discharge component should be steadily present in each moment of the recession. Sometimes, it is useful to use some conventional threshold to delineate the duration interval of an exponential flow component. Let us define this threshold here to be 1.0 L/s. Then, we can use Eq. 7.25 and set Q_t to be 1.0 L/s. For the two exponential flow components from Eq. 7.28, their duration ($t_{\mathrm{DUR-exponential1}}$ and $t_{\mathrm{DUR-}\mathit{I}\ \mathrm{exponential2}}$) then can be delineated as

$$t_{\mathrm{DUR-exponential1}} = \frac{\ln Q_t - \ln Q_{01}}{-\alpha_1} = \frac{\ln(1.0) - \ln(58.7)}{-0.005} = 814.5 \text{ days}$$

$$t_{\mathrm{DUR-}\mathit{e}\mathrm{exponential2}} = \frac{\ln Q_t - \ln Q_{02}}{-\alpha_2} = \frac{\ln(1.0) - \ln(174.9)}{-0.08} = 64.6 \text{ days}$$

Theoretically, the base flow (as the first exponential flow component is the most persistent flow component in the hydrograph) of this spring should last for 814.5 days until its discharge falls below 1.0 L/s. The second exponential flow component diminishes much more sooner; let us suppose within 65 days when it participates on the total discharge by less than 1.0 L/s.

Case study 4. Hydrograph separation into flow components—calculation of the representative time t_R, theoretically elapsed from the maximum discharge value Q_{max} for discharge value of Q_t

Hydrograph separation based on parameters of MRC described in Eq. 7.29 *is shown on the example of karstic spring Vítek in Chtelnica (Brezovské Karpaty Mts., Slovakia). As it is evident from* Eq. 7.29 *and* Fig. 7.15*, karstic groundwater discharged in the Vítek spring has a strong portion of the 1st exponential (slow-flow) component constantly present in the spring's discharge, while the quick-flow component (1st linear model component) appears only at high-flow periods when the total discharge exceeds ~30 L/s. The 2nd exponential flow component that is probably linked to groundwater circulation in opened fissures is regularly present in the total discharge, but only in small proportion. Its volume steeply rises in discharges of more than ~30 L/s. Still, nearly 85 % of the total volume of water is discharged in the 1st exponential flow component (sub-regime) that points to groundwater circulation in strongly fissured aquifer in dolomites.*

$$Q_t = 25.68e^{-0.0030t} + 7.66e^{-0.01t} + 9.52(1 - 0.04t) \tag{7.29}$$

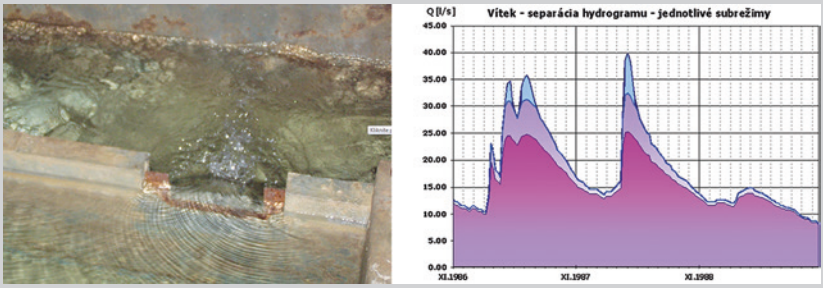

Fig. 7.15 Spring Vítek in Chtelnica (Brezovské Karpaty Mts., Slovakia), captured as a drinking water source (*left*, photograph from the database of the Slovak Hydrometeorological Institute). Its hydrograph separation into flow components using Eq. 7.29 (*right*)

Try to find out the how much of each flow component will be present in the discharge of 37.0 L/s and what relative portion of the second exponential flow component you will find in the discharge of 25.0 L/s in the spring Vítek.

Exercise

In MS Excel, use functions as in Case study 3, but change the input values in the «B» column to 0.003 ($B$1); 0.01 ($B$2); 0.04 ($B$3); and 0 ($B$4) for the recession coefficients as the second linear flow component is not described by Eq. 7.28. For starting discharges, change «B» column values

in the following way: $B$6 to 25.68; $B$7 to 7.66; $B$8 to 9.52; and $B$9 to zero (only one linear fast-flow component is present). Then, make the summation of all 3 existing flow components columns perhaps in the column «I», so that «I» = «E» + «F» + «G» in every row. Then, compare the values in the column «I» with the thresholds of 37.0 and 25.0 L/s.

In the first case, you will see that for time of 11 days the total discharge is 37.04 L/s, while for time of 12 days after the maximum, the total discharge is 36.52 L/s. This means that the representative time t_R for the discharge of 37.00 L/s ($t_{37.0}$) is somewhere between 11 and 12 days. Then, try to change the value in the column «D» unless the total discharge (column «I») in the same row is within an acceptable limit (the second decimal place). Here, $t_{37.0} = 11.08$ D. You were working manually instead of the described iteration process. You will see then that for $t_R = 11.08$ days, the first exponential component (column «E») would be 24.84 L/s (as it is $25.68 \cdot e^{-0.003 \cdot 11.8}$), the second exponential component (column «F») would be 6.86 L/s (as it is $7.66 \cdot e^{-0.01 \cdot 11.8}$) and the relative discharge of the only linear flow component would be 5.30 L/s (as it is equal to 9.52–9.52·0.04·11.08).

In the second case, we will find that for time of 66 days, the total discharge is 25.03 L/s, and for 67 days after the maximum, the total discharge would be 24.92 L/s. Again, the representative time t_R for the discharge of 25.00 L/s ($t_{25.0}$) should be somewhere between 66 and 67 days. After several trials to change the value in the column «D» unless the total discharge (column «I») in the same row would be within an acceptable limit (the second decimal place), we can estimate $t_{25.0}$ as 66.25 days. Then, that for $t_R = 66.25$ days, the first exponential component (column «E») would be 21.05 L/s ($=25.68 \cdot e^{-0.003 \cdot 66.25}$), the second exponential component (column «F») would be 3.95 L/s ($=7.66 \cdot e^{-0.01 \cdot 66.25}$) and the linear flow component would not exist at this moment.

The relative portion of the second exponential flow component would be then

$$3.95/25.00 = 16\%$$

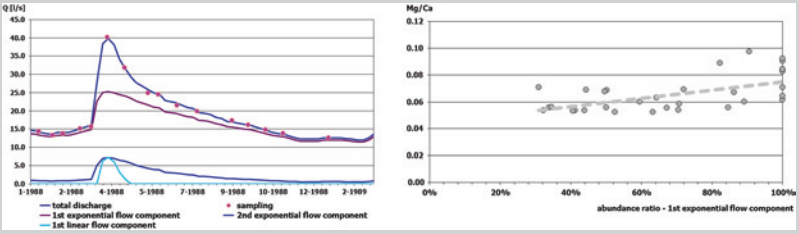

Fig. 7.16 Groundwater sampling of spring Vítek at various water stages with individual flow components differently represented (*left*). Correlation of Mg/Ca content ratio with relative abundance of the 1st exponential flow component (*right*)

In majority of cases, groundwater in a single sample can be considered as being a mixture of several water types of slightly different origin. This is even more evident in the case of karstic springs. Knowing that at every moment each measured discharge of a karstic spring is composed of superposition of two or more individual flow components, while only one flow component is usually present only during the driest period, we can try to link the results of water quality analyses with quantitative parameters. Proportional amounts of individual flow component discharges during the moment of sampling can be linked to the content of various (chemical) components present in the water sample. To obtain the end members of the theoretical mixture, if having sufficient number of samples taken at various water stages, we can perhaps try to link the relative representation of flow component in the total discharge with the analysed parameter (Fig. 7.16). To obtain the end member of the theoretical mixture corresponding to the "pure" (100 %) representation of the certain flow component, we only draw the forecast line based on statistical regression of flow component relative representation and parameter content up to the 100 % value. This is shown in Fig. 7.16, where the dissolved magnesium (Mg^{2+})/calcium (Ca^{2+}) ratio is correlated with the relative representation of the 1st exponential flow component to obtain estimation of the end member of 0.075 Mg/Ca ratio in this flow component, if existing as pure solution.

Reference:

Malík, P., Michalko, J., 2010. Oxygen Isotopes in Different Recession Subregimes of Karst Springs in the Brezovské Karpaty Mts. (Slovakia). Acta Carsologica 39, 2, 271–287

Different shapes of the spring's recession are attributed to drainage from different components of the groundwater system, reflecting karstification degree. For example, flatter parts of the recession curve may represent slow groundwater drainage of pores and micro fractures, which is characteristic of the 1st exponential flow component. This is described with an exponential equation having a smaller exponent. Portions of the hydrograph with a steeper slope are characteristic of enhanced karstification degree, with groundwater circulating in increasingly widened joints, bedding planes, fissures, and conduits, reflected by increasingly larger exponents of the exponential equations. Enhanced karstification degree and circulation in conduits is described by one or several linear equations. Several properties of the aquifer can be evaluated by recession curve analysis: the type of rock disruption or karstification degree, and the anticipated character of attenuation (self-purification) processes (Kullman 2000; Malík 2007; Malík and Vojtková 2012). The karstification degree of a recharge area derived from recession curve analysis can be an important feature determined. In the Table 7.8 *karstification degree is classified using a 10th-degree scale, 1st*

degree for the lowest karstification, 10th degree for best developed karstification. Differences in character of individual depletion hydrographs and resulting karstification degrees are also listed here. Karstification degree was primarily described by Kullman (1990) in 10 categories, later applied (Kullman 2000) for assessment of groundwater vulnerability in 10-degree ranking, later supplemented by Malík (2007) and Malík and Vojtková (2012) to cover all results of hydrograph analyses of springs and to refine more precisely defined parameters of depletion equations with the intention not to disturb previously defined classification.

References:

Kullman, E., 2000. Nové metodické prístupy k riešeniu ochrany a ochranných pásiem zdrojov podzemných vôd v horninových prostrediach s krasovo-puklinovou priepustnost'ou [New methods in groundwater protection and delineation of protection zones in fissure-karst rock environment; in Slovak]. Podzemná voda 6, 2,31–41.

Malík, P., 2007. Assessment of regional karstification degree and groundwater sensitivity to pollution using hydrograph analysis in the Velka Fatra Mts., Slovakia. Water Resources and Environmental Problems in Karst. Environ Geol 2007, 51. 707–711.

Malík, P., Vojtková, S., 2012. Use of recession-curve analysis for estimation of karstification degree and its application in assessing overflow/underflow conditions in closely spaced karstic springs. Environ Earth Sci 2012, 65, 2245–2257.

Table 7.8 Karstification degree in recharge areas of springs according to recession curves parameters (after Kullman 2000; Malík 2007; Malík and Vojtková 2012; supplemented and modified)

Karstification degree	Groundwater flow component type	Characteristic recession curve equation	Characteristics of recession curve parameters	Characteristics of karstification degree
0.5	Single exponential flow component, lower values of α_1	$Q_t = Q_{o1} \cdot e^{-\alpha 1 \cdot t}$	$\alpha_1 < 0.001$	Usually tectonic faults and shear zones filled with crushed material, with high buffering capability in relation to discharge. Mainly deeper groundwater circulation
1.0			$\alpha_1 = 0.001$ to 0.0025	
2.0	Single exponential flow component, higher values of α_1		$\alpha_1 = 0.0025$ to 0.007	Tectonic faults filled with crushed material with higher permeability and lower buffering capability in relation to discharge. In some cases deeper groundwater circulation
2.3			$\alpha_1 > 0.007$	
2.5	Combination of two or more merely exponential flow components characterised by different recession coefficients, lower values of α_1 and α_2	$Q_t = Q_{o1} \cdot e^{-\alpha 1 \cdot t} + Q_{o2} \cdot e^{-\alpha 2 \cdot t}$	$\alpha_1 < 0.0024$ and $\alpha_2 < 0.033$	Aquifer with dense, prevailingly regular fissure network, with majority of microfissures and small fissures. Increase in values α_1 and α_2 accompanies increasing permeability and also higher heterogeneity of fissured rock environment
2.7			$\alpha_1 < 0.0024$ or $\alpha_2 < 0.033$	
3.0			$\alpha_1 = 0.0024$ to 0.0045; $\alpha_2 = 0.033$ to 0.067	
3.5	Combination of two or more merely exponential flow components' flow characterised by different recession coefficients, higher values of α_1 and α_2		$\alpha_1 = 0.0024$ to 0.0043 and $\alpha_2 = 0.060$ to 0.16	Aquifer with irregularly developed fissure network, with majority of open macrofissures, also with possible presence of karst conduits of limited extent. In extreme cases, even short-term turbulent flow might occur in this type of rock environment
3.7			$\alpha_1 > 0.0043$ and $\alpha_2 < 0.060$	
4.0			$\alpha_1 = 0.0041$ to 0.018 and $\alpha_2 = 0.055$ to 0.16	

(continued)

Table 7.8 (continued)

Karstification degree	Groundwater flow component type	Characteristic recession curve equation	Characteristics of recession curve parameters	Characteristics of karstification degree
4.3	Discharge hydrograph is composed of linear model flow component and unexponential flow component. Substantial role in groundwater discharge plays the exponential flow component	$Q_t = Q_{o1} \cdot e^{-\alpha 1 \cdot t} + Q_{o4} \cdot (1 - \beta_1 \cdot t)$	$\alpha_1 > 0.018$ or $\alpha_2 > 0.16$	Aquifer with anticipated existence of crushed water-bearing zone (e.g. fault zone) or by dense network of open small fissures in combination with simple, partly (or occasionally) phreatic conduit system of considerable extent (e.g. with open karstified fault in the vadose zone)
4.7			$\alpha_1 > 0.018$ and $\alpha_2 > 0.16$	
5.0			β and α—low values	
5.5	Complex discharge regime, a combination of one linear model flow component and two exponential flow components. Discharging of linear model flow component is of short-term influence in comparison with overall groundwater discharge	$Q_t = Q_{o1} \cdot e^{-\alpha 1 \cdot t} + Q_{o2} \cdot e^{-\alpha 2 \cdot t} + Q_{o4} \cdot (1 - \beta_1 \cdot t)$	$\alpha_1 > 0$ and $\alpha_2 > 0$ and $\beta_1 > 0$	Extensive disruption and disintegration of rock environment, with majority of open, medium-sized, both not karstified and karstified fissures in the phreatic zone of the fissure karst aquifer (according to α_1) and with smaller influence of connected conduits (groundwater of large karstic channels, according to ß$_1$)
6.0	Very complex discharge regime, a combination of two linear model flow components and two exponential flow components. Discharges of linear model flow components are of short-term influence in comparison with overall groundwater discharge	$Q_t = Q_{o1} \cdot e^{-\alpha 1 \cdot t} + Q_{o2} \cdot e^{-\alpha 2 \cdot t} + Q_{o4} \cdot (1 - \beta_1 \cdot t) + Q_{o5} \cdot (1 - \beta_2 \cdot t)$	β_2, β_1 and α_1, α_2—high values	Extensive disruption and disintegration of rock environment, with majority of open, medium-sized, both not karstified and karstified fissures in the phreatic zone of the fissure karst aquifer (according to α_1) and with smaller influence of connected conduits (groundwater of large karstic channels, according to ß$_1$ and ß$_2$)

(continued)

Table 7.8 (continued)

Karstification degree	Groundwater flow component type	Characteristic recession curve equation	Characteristics of recession curve parameters	Characteristics of karstification degree
7.0	Discharge regime is a combination of one exponential flow component and two to three flow components with linear flow model. Substantial role in groundwater discharge plays the exponential flow component	$Q_t = Q_{o1} \cdot e^{-\alpha 1 \cdot t} + Q_{o4} \cdot (1-\beta_1 \cdot t) + Q_{o5} \cdot (1-\beta_2 \cdot t) + Q_{o6} \cdot (1-\beta_3 \cdot t)$	β_3, β_2, β_1 and α—high values, $\beta_1 > \beta_2$	Developed karstification of the aquifer, formed by large open tectonic faults and karstic channels, as well as by significant portion of karstified and non-karstified fissures and microfissures in rock blocks, generating phreatic zone with karstic groundwater table
8.0	Discharge regime is a combination of unexponential flow component with two to three linear model flow components. Substantial role in groundwater discharge is played by linear model flow components. Exponential flow component is less significant		β_3, β_2, β_1 and α—high values	Highly developed karstification of the aquifer, formed by large open conduits (karst channels). Presence of open active small fissures and microfissures is reduced. Circulation of substantial part of groundwater is mainly via preferred pathways of channel systems. Phreatic zone is missing or its role is insignificant
8.5	Flow regime that is represented merely by linear flow model, as the only one flow component present, which represents linear circulation in channel systems (conduits) without hydraulic connection to groundwater in adjacent rock blocks. Groundwater circulation is mostly connected to vadose zone	$Q_t = Q_{o4} \cdot (1 - \beta_1 \cdot t)$	α_1; $\alpha_2 = 0$ and $\beta_1 > 0$	Karstic aquifer with well-developed conduit system, without any significant connection to open phreatic fissure systems in adjacent rock blocks. Extensively developed conduit system can ensure permanent groundwater replenishment

(continued)

Table 7.8 (continued)

Karstification degree	Groundwater flow component type	Characteristic recession curve equation	Characteristics of recession curve parameters	Characteristics of karstification degree
9.0	Flow regime, represented merely by two linear flow components. These represent linear circulation in channel systems (conduits) without hydraulic connection to groundwater in adjacent rock blocks. Groundwater circulation is mostly connected to vadose zone	$Q_t = Q_{o4} \bullet (1 - \beta_1 \bullet t) + Q_{o5} \bullet (1 - \beta_2 \bullet t)$	β_1, β_2—low values	Karstic aquifer with well-developed conduit systems of karstic groundwater pathways, without any significant connection to open phreatic fissure systems in adjacent rock blocks. Replenishment of groundwater resources can still be ensured by extensively developed conduit system
10.0	Complex discharge regime, consisting of three different linear flow components. Probability of a very complex groundwater circulation by occasional flows in the vadose zone. Documented only in perennial flows	$Q_t = Q_{o4} \bullet (1 - \beta_1 \bullet t) + Q_{o5} \bullet (1 - \beta_2 \bullet t) + Q_{o6} \bullet (1 - \beta_3 \bullet t)$	β_1, β_2 and β_3—high values	Karstic aquifer with extensive conduit system, without any significant connection to open phreatic fissure systems in adjacent rock blocks. In its spatial extent, the conduit system is bound only to the vadose zone, without enabling permanent groundwater replenishment

References

Alfaro C, Wallace M (1994) Origin and classification of springs and historical review with current applications. Environ Geol 24:112–124

Barnes BS (1939) The structure of discharge recession curves. Trans Am Geophys Union 20:721–725

Bonacci O (2001) Analysis of the maximum discharge of karst springs. Hydrogeol J 2001(9):328–338

Bonacci O (2011) Karst springs hydrographs as indicators of karst aquifers. Hydrol Sci (Journal des Sciences Hydrologiques) 38(1–2):51–62

Bonacci O, Bojanic D (1991) Rythmic karst spring. Hydrol Sci (Journal des Sciences Hydroloqiques) 36(1–2):35–47

Boussinesq J (1877) Essai sur la théorie des eaux courantes do mouvement non permanent des eaux souterraines. Acad Sci Inst Fr 23:252–260

Boussinesq J (1903) Sur un mode simple d'écoulement des nappes d'eau d'infiltration à lit horizontal, avec rebord vertical tout autour lorsqu'une partie de ce rebord est enlevée depuis la surface jusqu'au fond. C R Acad Sci 137:5–11

Boussinesq J (1904) Recherches théoriques sur l'écoulement des nappes d'eau infiltrées dans le sol et sur le débit des sources. J Math Pure Appl 10(5):5–78

Dewandel B, Lachassagne P, Bakalowicz M, Weng Ph, Al-Malki A (2003) Evaluation of aquifer thickness by analysing recession hydrographs. Application to the Evaluation Oman ophiolite hard-rock aquifer. J Hydrol 274:248–269

Drogue C (1972) Analyse statistique des hydrogrammes de décrues des sources karstiques. J Hydrol 15:49–68

Dub O, Němec J (1969) Hydrologie. Česká matice technická, LXXIV (1969), 353, Technický průvodce 34, SNTL – Nakladatelství technické literatury, Praha, p 378

Fiorillo F (2011) Tank-reservoir drainage as a simulation of the recession limb of karst spring hydrographs. Hydrogeol J 2011(19):1009–1019

Flora SP (2004) Hydrogeological characterization and discharge variability of springs in the Middle Verde River watershed, Central Arizona. MSc thesis, Northern Arizona University, p 237

Forkasiewicz J, Paloc H (1967) Le régime de tarissement de la Foux de la Vis. Etude préliminaire. AIHS Coll. Hydrol.des roches fissurées, Dubrovnik (Yugoslavia) 1: 213–228

Foster HA (1924) Theoretical frequency curves and their application to engineering problems. Am Soc Civil Eng Trans 87:142–303

Foster HA (1934) Duration curves. Am Soc Civil Eng Trans 99:1213–1267

Gregor M (2008) Vývoj programov na analýzu časových radov výdatností prameňov a prietokov vodných tokov. (Software development for time-series analysis of springs yields and river discharges; in Slovak). Podzemná voda 14/2:191–200

Gregor M, Malík P (2012) Construction of master recession curve using genetic algorithms. J Hydrol Hydromechanics 60(1):3–15

Griffiths GA, Clausen B (1997) Streamflow recession in basins with multiple water storages. J Hydrol 190:60–74

Hall FR (1968) Base-flow recessions—a review. Water Resour Res 4(5):973–983

Király L (2003) Karstification and groundwater flow/Speleogenesis and evolution of karst aquifers. In: Gabrovšek F (ed) Evolution of karst: from prekarst to cessation. Zalozba ZRC, Postojna-Ljubljana, pp 155–190

Kovács A (2003) Geometry and hydraulic parameters of karst aquifers—a hydrodynamic modelling approach. PhD thesis, La Faculté des sciences de l'Université de Neuchâtel, Suisse, p 131

Kovács A, Perrochet P, Király L, Jeannin PY (2005) A quantitative method for the characterisation of karst aquifers based on spring hydrograph analysis. J Hydrol 303:152–164

Kullman E (1980) L'evaluation du regime des eaux souterraines dans les roches carbonatiques du Mésozoique des Carpates Occidentales par les courbes de tarissement des sources.

Geologický ústav Dionýza Štúra, Bratislava, Západné Karpaty, sér. Hydrogeológia a inžinierska geológia 3:7–60
Kullman E (1990) Krasovo-puklinové vody (Karst-fissure waters; in Slovak). Geologický ústav Dionýza Štúra, Bratislava, p 184
Kullman E (2000) Nové metodické prístupy k riešeniu ochrany a ochranných pásiem zdrojov podzemných vôd v horninových prostrediach s krasovo-puklinovou priepustnosťou (New methods in groundwater protection and delineation of protection zones in fissure-karst rock environment; in Slovak). Podzemná voda 6/2:31–41
Kresic N (2007) Hydrogeology and groundwater modeling, 2nd edn. CRC Press/Taylor and Francis, Boca Raton
Lamb R, Beven K (1997) Using interactive recession curve analysis to specify a general catchment storage model. Hydrol Earth Syst Sci 1(1):101–113
Maillet E (ed) (1905) Essais d'hydraulique soutarraine et fluviale vol 1. Herman et Cie, Paris, p 218
Malík P (2007) Assessment of regional karstification degree and groundwater sensitivity to pollution using hydrograph analysis in the Velka Fatra Mts., Slovakia. Water Resources and environmental problems in karst. Environ Geol 51:707–711
Malík P, Michalko J (2010) Oxygen isotopes in different recession subregimes of karst springs in the Brezovské Karpaty Mts. (Slovakia). Acta Carsologica 39(2):271–287
Malík P, Vojtková S (2012) Use of recession-curve analysis for estimation of karstification degree and its application in assessing overflow/underflow conditions in closely spaced karstic springs. Environ Earth Sci 65:2245–2257
Mangin A (1969) Etude hydraulique du mecanisme d'intermittence de Fontestorbes (Belesta, Ariege). Annales de Speleologie 24(2):253–298
Meinzer OE (1923a) Outline of ground-water hydrology. USGS Water-Supply Paper, p 494
Meinzer OE (1923b) The occurrence of ground water in United States with a discussion of principles. USGS Water-Supply Paper, 489, Washington DC, p 321
Milanovic PT (1981) Karst hydrogeology. Water Resources Publications, Littleton
Netopil R (1971) The classification of water springs on the basis of the variability of yields. Studia Geographica 22:145–150
Oraseanu I, Iurkiewicz A (2010) Calugari ebb and flow spring. In: Oraseanu I, Iurkiewicz A (eds) Karst hydrogeology of Romania. Belvedere Publishing, Oradea, pp 262–274
Padilla A, Pulido Bosch A, Mangin A (1994) Relative importance of baseflow and quickflow from hydrographs of karst spring. Ground Water 32:267–277
Posavec K, Bačani A, Nakić Z (2006) A visual basic spreadsheet macro for recession curve analysis. Ground Water 44(5):764–767
Rutledge RT (1998) Computer programs for describing the recession of groundwater discharge and for estimating mean groundwater recharge and discharge from stream flow records-update. USGS water-resource investigations report 98-4148. Reston, VG
Searcy JK (1959) Flow-duration curves. manual of hydrology, part 2. Low-flow techniques. Geological survey water-supply paper 1542-A, Methods and practices of the geological survey, United States Government Printing Office, Washington, p 33
Schöeller H (1948) Le régime hydrogéologique des calcaires éocénes du Synclinal du Dyr el Kef (Tunisie). Bull Soc Géol Fr 5(18):167–180
SÚTN (2009) Slovak technical standard STN 751520 Hydrológia, Hydrologické údaje podzemných vôd, Kvantifikácia výdatnosti prameňov. (Hydrology, hydrological data on groundwater, quantification of spring's discharge; in Slovak), Slovenský ústav technickej normalizácie (SÚTN) Bratislava, p 14
Springer AE, Stevens LE, Anderson DE, Parnell RA, Kreamer DK, Flora SP (2004) A comprehensive springs classification system: integrating geomorphic, hydrogeochemical and ecological criteria. In: Aridland springs in North America: ecology and conservation, pp 49–75
Tallaksen LM (1995) A review of baseflow recession analysis. J Hydrol 165:349–370

Tallaksen LM, van Lanen HAJ (eds) (2004) Hydrological drought, processes and estimation methods for streamflow and groundwater. Developments in Water Science, vol 48. Amsterdam, Elsevier Science B.V., p 579

Toebes C, Strang DD (1964) On recession curves 1: recession equations. J Hydrology (New Zealand) 3/2:2–15

Werner PW, Sundquist KJ (1951) On the groundwater recession curve for large watersheds. IAHS Publ 33:202–212